A&A 571, A63 (2014)
DOI: 10.1051/0004-6361/201424329

Astronomy & Astrophysics

New catalogue of one-apparition comets discovered in the years 1901–1950

I. Comets from the Oort spike⋆

Małgorzata Królikowska[1], Grzegorz Sitarski[1], Eduard M. Pittich[2], Sławomira Szutowicz[1], Krzysztof Ziołkowski[1], Hans Rickman[1,3], Ryszard Gabryszewski[1], and Bożenna Rickman[4]

[1] Space Research Centre of the Polish Academy of Sciences, Bartycka 18A, 00-716 Warsaw, Poland
e-mail: [mkr;sitarski;slawka;kazet;kacper]@cbk.waw.pl
[2] Astronomical Institute of the Slovak Academy of Sciences, 845 04 Bratislava, The Slovak Republic
e-mail: pittich@savba.sk
[3] Department of Physics and Astronomy, Uppsala University, Box 516, 75120 Uppsala, Sweden
e-mail: Hans.Rickman@physics.uu.se
[4] Former employee of Space Research Centre of the Polish Academy of Sciences, Bartycka 18A, 00-716 Warsaw, Poland

Received 3 June 2014 / Accepted 3 September 2014

ABSTRACT

Context. The orbits of one-apparition comets discovered in the early part of the last century have formerly been determined with very different numerical methods and assumptions on the model of the solar system, including the number of planets taken into account. Moreover, observations of the comet-minus-star-type sometimes led to determination of the comet position that are less precise than what we can derive today by using a more modern star catalogue.
Aims. We aim to provide a new catalogue of cometary orbits that are derived using a completely homogeneous data treatment, accurate numerical integration, and a modern model of the solar system.
Methods. We collected the complete sets of observations for investigated comets from the original publications. Then we recalculated the cometary positions for the comet-minus-star-type of observations using the Positions and Proper Motions Star Catalogue, and applied a uniform method for the data selection and weighting. As a final result, new osculating orbits were determined. Secondly, dynamical calculations were performed to the distance of 250 AU from the Sun to derive original and future barycentric orbits for evolution backward and forward in time. These numerical calculations for a given object start from a swarm of virtual comets constructed using our osculating (nominal) orbit. In this way, we obtained the orbital element uncertainties of original and future barycentric orbits.
Results. We present homogeneous sets of orbital elements for osculating, original, and future orbits for 38 one-apparition comets. Non-gravitational orbits are derived for thirteen of them.

Key words. catalogs – comets: general – Oort Cloud

1. Introduction

The idea of a new catalogue of one-apparition comets was first conceived in the mid-1960s by a team of three astronomers from Warsaw, Maciej Bielicki (1906–1988), Grzegorz Sitarski, and Krzysztof Ziołkowski. The latter two were young enthusiasts of the new computing capabilities that in the first half of the sixties appeared on the horizon for Polish astronomers by gaining access to computers that were called electronic mathematical machines. Bielicki, Sitarski and Ziołkowski began a very long-term project to create and develop a unified package of numerical codes that would perform a fully automated orbital integration of the motion of comets and asteroids to determine their orbits on the basis of astrometric data and investigate their dynamical evolution on any time scales. The numerical codes were gradually verified with examples of comets (e.g. 22P/Kopff, 26P/Grigg-Skjellerup), which in turn led to the start of the catalogue project in 1967. This was a very ambitious task in that time in Poland.

The previously existing cometary catalogues contained orbital elements of comets derived from a variety of sources, which means that different methods were used that are characterized by different accuracy and assume different models of the solar system. This new catalogue, in contrast, would contain a uniform set of orbital elements obtained using modern numerical methods and a modern ephemeris of the solar system. The second main idea behind the new catalogue was to determine the orbits of each comet using all the existing positional observations.

Therefore, the most important problems to solve were

– completing all the comet observations in astronomical literature; at that time there was no internet, and it was difficult to access to several of the original publications containing the old observations;
– reducing collected measurements to a single star-catalogue when possible and selecting and weighting these measurements on the basis of mathematically objective criteria;

⋆ All catalogue tables given in appendices (Tables A.1–E.1) are also available at the CDS via anonymous ftp to cdsarc.u-strasbg.fr (130.79.128.5) or via http://cdsarc.u-strasbg.fr/viz-bin/qcat?J/A+A/571/A63

– developing the methods for determining the osculating orbits of comets in a uniform manner with the use of accurate numerical integration and a modern model of the solar system.

Thanks to Eduard Pittich from the Astronomical Institute of the Slovak Academy of Sciences at Bratislava, the cooperation between Polish and Slovak astronomers was established for the catalogue project during the twelfth plenary meeting of COSPAR held in Prague in May 1969. Information about this project and the preliminary theoretical solutions of various problems related to data processing and orbital calculations were presented and discussed in a larger international group of specialists during the IAU symposium 45, "The Motion, Evolution of Orbits, and Origin of Comets" held in Leningrad (now Saint Petersburg) in August 1970. The early publications that directly referred to the idea of a new catalogue outlined how important it would be to uniformly treat astrometric observations and the way they would be selected and weighted (Bielicki 1972; Sitarski 1972; Bielicki & Ziołkowski 1976). These also described the data treatment and the recurrent power-series method of numerical integration developed by Sitarski (1979a,b).

The Polish-Slovak cooperation focused mainly on collecting positional observations of one-apparition comets. In Poland, the data were collected from the first half of the twentieth century. This activity involved many young astronomers, students, and amateur astronomers, and their work was first coordinated by Tomasz Chlebowski, then still a student of astronomy, and next by Wanda Borodziewicz from the Space Research Centre PAS. In the Chech and Slovak Republics (former Czechoslovakia), where the astronomical libraries had not been as badly destroyed during the Second World War as in Poland, astronomers collected the data for comets of the nineteenth century.

A database of cometary positional observations from the first half of the twentieth century and the development of basic numerical codes associated with the Catalogue project was almost completed in October 1988. At that time, the Polish-Slovak conference "The dynamics of small bodies in the solar system" took place in Warsaw and was largely devoted to the catalogue of one-apparition comets.

Then there was a period of inactivity in the formal work on the catalogue, but the software packages for the orbital calculation were still improved and upgraded for the current dynamical studies of small bodies in the solar system. The adopted research methods, including the method of numerical integration and model of the solar system, were described by Sitarski (1984, 1989, 2002). The developed methods and software packages have been thoroughly tested during all these years, with a resulting number of publications examining the motion of both asteroids and comets, including the non-gravitational effects, for example, Sitarski (1992, 1998) and Rickman et al. (1987).

The final coherent and homogeneous study conducted to determine the orbital motion of comets of the first half of the twentieth century, which is the basis of this part I of the catalogue of one-apparition comets, was carried out during the years 2009–2013.

The paper is organized as follows: in the next section we describe the sample of comets and the data collected for all these objects. Data processing and orbit determination are described in Sect. 3. In some cases we were able to determine the non-gravitational (hereafter NG) orbits. Therefore in Sect. 4, we briefly describe the adopted model of NG acceleration and give some examples of how these NG solutions fit the data in comparison to pure gravitational models. Original and future orbits are discussed in Sect. 5. The article ends with a brief discussion (Sect. 6).

This publication is additionally accompanied by an online catalogue available at `ssdp.cbk.waw.pl/LPCs`, providing entries for orbital elements of individual comets and for full swarms of the original and future virtual comets (VCs; see Sect. 5) that formed the basis for the detailed analysis of the dynamical evolution. In the future, we plan to insert more graphics there, for example O–C time variations.

1.1. Brief description of the catalogue

The main part of this catalogue, that is, the tabular material given in this publication, consists of seven tables.

– Tables A.1–A.2 describe the collected observational data and how they were processed,
– Tables B.1–B.2 present homogeneous sets of heliocentric osculating orbits of all investigated comets and sets of non-gravitational parameters for comets with determinable non-gravitational solutions,
– Table C.1 lists the original and future barycentric inverse semi-major axes and the orbit quality assessment,
– Tables D.1–E.1 include barycentric sets of original and future orbits determined at 250 AU from the Sun.

2. Sample and general data characteristics

For this new catalogue we investigated only comets that were discovered in the first half of the twentieth century. The Catalogue of Cometary Orbits (Marsden & Williams 2008, hereafter MW08) includes 93 long-period comets (orbital period greater than 200 yr) and 33 parabolic comets (assumed $e = 1$) discovered in this period.

For the first part of the catalogue, we constructed a sample of near-parabolic comets with original semi-major axes of $1/a_{\rm ori} < 0.000130\,{\rm AU}^{-1}$ in MW08, that is, comets of original semi-major axes larger than ~7700 AU. This means that we limited ourselves here to comets of good-quality orbits as defined by MW08, that is, according to the orbital quality assessment introduced by Marsden et al. (1978, hereafter MSE). We found 38 comets of $1/a_{\rm ori} < 0.000130\,{\rm AU}^{-1}$ in MW08, 32 of which have first-class-quality orbits (class 1A or 1B), and the remaining 6 have second-class-quality orbits (2A or 2B). In this sample, only six comets have a perihelion distance larger than 3.0 AU, and the highest value is $q_{\rm osc} = 4.2$ AU (comet C/1925 F1). The remaining comets from the years 1901–1950 will be the subject of part II of the catalogue. At the moment we have analysed only about 30% of the objects from this second part.

The positional data for all selected comets were collected from the literature many years ago in Warsaw in cooperation with the Slovakian group from the Astronomical Institute in Bratislava. All collected data are plotted in Fig. 1, where significant selection effects are easily visible, such as the striking predominance of northern sky observations. Characteristics of the collected observational material are given in Cols. (4)–(7) of Table A.1, while the data interval and number of measurements taken to determine the orbit in MW08 are shown in Cols. (8)–(9). In most cases the comets were discovered before perihelion passage, but some were detected just after passing through perihelion (marked as "post" data arc in Col. (4) of Table A.1). Moreover, many comets were followed to much larger heliocentric distances than the heliocentric distance at discovery. This

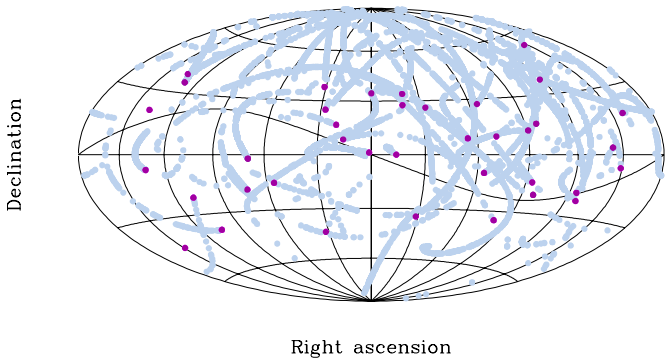

Fig. 1. Overall view on cometary tracks filled by collected astrometric observations in geocentric equatorial coordinate system given in Aitoff projection. The declination is plotted along the ordinate, the right ascension along the abscissa (increasing from zero to 360 degree from the left to right) and the centre of projection is 0°of declination and 180° of right ascension. The lines of right ascension and declination are shown at 30° intervals, and the wavy line shows the projection of the ecliptic onto the celestial sphere. Each positional observation is shown as a light steel-blue point for a given comet, except for the first observation, which is shown as a dark magenta point.

asymmetry in observed heliocentric distances around perihelion is easily visible in Col. (7) of Table A.1. Only in ten cases the heliocentric distance at the moment of discovery is similar to that of the last measurement of the cometary position. For example, only two comets, C/1906 E1 and C/1916 G1, were discovered at distances greater than 5.0 AU from the Sun, while 12 comets were still observed after perihelion passage at similarly large heliocentric distances.

In most cases, we have more observations than the observation sets that were taken to determine the orbits presented in MW08 (compare Cols. (5) and (9) of Table A.1)[1]. Only in two cases (C/1906 E1, C/1942 C1) we found fewer literature data than declared in MW08 (Col. (3) of Table C.1).

Comet C/1906 B1 is a special case. In 2003 Kronk (2008) identified two prediscovery observations of this comet. He found that an unknown comet photographed by E. E. Barnard in July 1905 is the comet discovered in January 1906 by Brooks. These observations extend the data interval by about six months. Williams (2005) calculated the orbital elements of the comet based on the completed set of observations (arc of nine months, see also MW08). We supplemented our data for this comet with some positional observations available at the MPC archive (IAU Minor Planet Center Database 2013).

Comet C/1940 R2 is the second special case in this context. We were able to find more data than in MW08 for this comet but, unfortunately, all of them were taken before 1941 April 1, whereas in MW08 the data sequence continues to June 17.

In the remaining cases, however, we have richer observational materials than those listed in MW08 for orbit determination. In many cases, our collected data are even several times more numerous, for instance for comets C/1902 R1, C/1902 X1, C/1904 Y1, C/1912 R1, C/1913 Y1, C/1914 F1, C/1919 Q2, C/1932 M1, C/1937 C1, and C/1950 K1. Moreover, for almost all comets we also have data of comet-minus-star type that allow us to correct the cometary positions for a newer catalogue than was formerly available. Starting with orbit determination in this project, we decided to use the Positions and Proper Motions Star Catalogue (PPM catalogue) that is the successor of the SAO catalogue and contains precise positions (in the J2000/FK5 coordinate system) of almost 400 000 stars located on the whole sky and is almost complete to $V = 9\overset{m}{.}5$ with about 25 per cent of stars fainter than $V = 10^m$. The PPM catalogue was very helpful for finding the star positions for the purpose of very old observations of comets (Gabryszewski 1997). During this project we found that it is also very helpful for the sample of comets discovered in the years 1901–1950 (see next section).

3. Data processing and osculating-orbit determination

Old cometary observations were prepared by observers as apparent positions in right ascension and declination or as reduced positions for the epoch of the beginning of the year of a given observation; the observations were much more rarely reduced to a more distant epoch. This is a huge advantage of these data, because we were able to uniformly take into account all necessary corrections associated with the data reduction to the standard epoch.

Moreover, as was already mentioned, many observers have also published the comet-minus-star measurements, (☄-★). Thus, the most original observations of a comet's positions relative to the reference stars have allowed us to recalculate new positions of the comet using a more modern star catalogue (PPM catalogue).

This caused the data processing and each cometary orbit determination to consist of three steps.

At the beginning of the first step we determined the preliminary pure gravitational (hereafter GR) osculating orbit using only a selection procedure based on Chauvenet's criterion (fewer than one hundred observations in the given set of data) or Bessell's criterion (more than one hundred observations). For a description of these two criteria, see Bielicki & Sitarski (1991) and Królikowska et al. (2009). Next, we extracted all measurements with comet-minus-star (☄-★) data. The numbers of this type of observations are given in Col. (2) of Table A.2. Assuming that the (☄-★) data are measurements that cannot be changed, we recalculated the new comet position for these observations in right ascension and declination using the PPM catalogue. The detailed procedure to recalculate the comet's position is described by Gabryszewski (1997), where the successful application to four sets of cometary measurements taken between the years 1860–1930 is also presented. In all cases we found that this procedure improved the orbit determination by (i) reducing the root mean square (rms) residual and/or by (ii) changing the number of residuals. This can be seen by comparing rms and number of residuals for the osculating orbit determined from the whole set of measurements (Col. (5) of Table A.1) before applying the PPM procedure (Cols. (5)–(6) of Table A.2) with rms and number of residuals after the PPM-procedure application (Cols. (7)–(8) of Table A.2). The recalculated cometary positions were selected using the same criterion

[1] In many old astrometric measurements the position of a comet in right ascension, α, and declination, δ, was taken at times separated by a few to several tens of minutes. Then the single observation contains only α or δ. We used such a measurement in one coordinate as a separate observation with one residual where the second residual was rejected for obvious reasons. Generally, we accepted rejection in only one coordinate, α or δ, in our selection procedure when the second coordinate was incorrect. Thus, it is more appropriate to compare the number of residuals taken for our orbit determination (Col. (10) of Table C.1) with those listed in MW08 (taking twice as many data as given in Col. (9) of Table A.1).

and procedure as for the original data. For example, the rms for comets C/1903 M1 (59% of (➹-★) data improved spectacularly: the rms decreased from 4.″39 to 3.″76), as well as for C/1907 E1 (72%, 4.″14 ↘ 2.″82), for C/1919 Q2 (75%, 3.″38 ↘ 2.″58), for C/1932 M1 (48%, 3.″52 ↘ 2.″89), and for C/1937 C1 (45%, 4.″42 ↘ 3.″49).

We also collected many data consisting of only (➹-★) measurements, that is, without calculated cometary positions. In these situations we interpolated a preliminary comet position from the observations taken just before and after such a measurement. Using this preliminary position of the comet, we tried to find the actual star position on the basis of the PPM catalogue and then the actual comet position. In some cases this method was successful and allowed us to significantly increase the number of data, as in the case of C/1916 G1 (number of residuals increased by 10%), C/1921 E1 (11%) and C/1922 U1 (12%); these three cases are marked by the icon ➹ in Col. (8) of Table A.2).

At the end of this step we determined the osculating orbit from data modified following the PPM catalogue, using the pure selection procedure based on Chauvenet's or Bessel's criterion (depending on the number of measurements in the data set, as mentioned before). Additionally, when there were very many data, we selected data before and after perihelion passage, independently. This is a very good way to select data to estimate the possibility of detecting NG effects in the cometary motion. When the rms derived from the whole data set using the pure GR model exceeds the rms for the two legs of the GR orbit determined independently, this indicates that the NG effects will be easily determinable in the motion of the comet.

In the second step we determined the osculating orbit from the data recalculated following the PPM catalogue, using the selection and weighting procedure simultaneously with the orbit determination. We found earlier that the weighting procedure is crucial for the orbit fitting (see for example Królikowska et al. 2009; Królikowska & Dybczyński 2010). Here, we confirm this conclusion also for comets discovered in the first half of the twentieth century. We decided, however, not to weight observations for smaller data sets (fewer than one hundred measurements). Thus, the data were not weighted for C/1914 M1, C/1940 S1, C/1944 K2, and C/1948 T2. We made an exception for C/1942 C2, where the model presented here was weighted since the observations were taken only at four different observatories. Generally, the weighting procedure results in lower rms; for C/1902 X1, for example, the rms decreased from 3.″37 (1301 residuals, preliminary solution, see Col. (7) of Table A.2) to 1.″66 (1307 residuals, Col. (9) of Table C.1), for C/1916 G1 from 3.″14 (826 residuals) to 1.″97 (823 residuals, GR solution), or for C/1942 C2 from 1.″65 (88 residuals) to 1.″57 (88 residuals).

Additionally, in some special cases we used a more restrictive criterion of data selection for the final solution than for the preliminary solution. The final non-weighted solution for C/1940 S1 (the poorest quality of orbit in this catalogue), for example, was based on data selected according to Bessel's criterion, and the resulting rms is significantly lower than the preliminary one (compare Col. (9) of Table C.1 and Col. (7) of Table A.2).

The rms and number of residuals resulting from the final selection and weighting procedure are given in Cols. (9)–(10) of Table C.1, while elements of these pure GR osculating orbits are listed in Table B.1. Our data processing resulted in reasonably few residual rejections in comparison to MW08 (compare Col. (10) of Table C.1 with twice as many observations given in Col. (10) of Table A.1). Our selecting and weighting procedure gives fewer than 22% of rejected residuals for comets investigated here, and the mean percentage of rejected residuals is 17.6. The estimates of data percentage used for osculating orbits listed in MW08 are shown in Col. (3) of Table C.1, where numbers are given in comparison to data sets collected and used in this investigation. Except for the two comets already mentioned in Sect. 2 (C/1906 E1 and C/1942 C1), these percentages taken into account to determine the orbit are significantly lower than ours, below 50% for 20 comets, and even below 30% for five of them.

Table C.1 also includes the general quality characteristics of the osculating-orbit determinations. The orbit quality assessment given in MW08 and taken according to the original MSE method is presented in Col. (2). The same MSE method applied to our solution of osculating orbits leads to a different orbit quality assessment for comets C/1902 X2 (1A instead of 1B) C/1906 E1 (1A instead of 1B), C/1914 M1 (1B instead of 1A) C/1940 S1 (2A instead of 2B), C/1941 K1 (1A instead of 1B), and C/1942 C1 (1A instead of 1B), where we compare the MW08 orbit quality with our pure GR solution (see Col. (11) of Table C.1). In almost all these cases our osculating orbits are of better quality according to the MSE method of orbit quality assessment. In Col. (12) of Table C.1 we list the new quality assessment introduced by Królikowska & Dybczyński (2013). This new orbit quality estimate is based on the original MSE method, but is slightly more restrictive and better diversifies than the MSE method, especially concerning recently discovered objects that are observed using modern techniques. In the following discussion, we refer to this new orbit quality estimate.

In the third step we made an attempt to determine the NG effects in the motion of each comet. Once again, each individual set of astrometric data was selected and weighted simultaneously with the iterative process of NG orbit determination. The model of NG motion is described in the next section. In the present investigation we were able to determine NG effects in the motion of thirteen comets, that is, in 34% of the comets investigated here. These comets are indicated by grey shading in Table A.1.

All the numerical calculations presented here are based on the Warsaw ephemeris DE405/WAW (Sitarski 2002), that is, a numerical solar system ephemeris, which is consistent at a high accuracy with the JPL ephemeris DE405 (Standish 1998). The equations of motion were integrated using the recurrent power-series method (Sitarski 1989), taking into account the perturbations by all planets and including relativistic effects.

4. Non-gravitational acceleration

To determine the NG cometary orbit we applied the standard formalism proposed by Marsden et al. (1973, hereafter MSY) where the three orbital components of the NG acceleration acting on a comet are expressed by a function $g(r)$ symmetric relative to perihelion,

$$F_i = A_i g(r), \quad A_i = \text{const. for} \quad i = 1, 2, 3, \tag{1}$$

$$g(r) = \alpha\,(r/r_0)^{-2.15}\left[1 + (r/r_0)^{5.093}\right]^{-4.614}, \tag{2}$$

where F_1, F_2, F_3 represent the radial, transverse, and normal components of the NG acceleration, respectively, and the radial acceleration is defined outward along the Sun-comet line. The normalization constant $\alpha = 0.1113$ gives $g(1\ \mathrm{AU}) = 1$; the scale distance $r_0 = 2.808$ AU. From orbital calculations, the NG parameters A_1, A_2, and A_3 were derived together with six orbital elements within a given time interval (numerical methods were originally described by Sitarski 1984). The standard

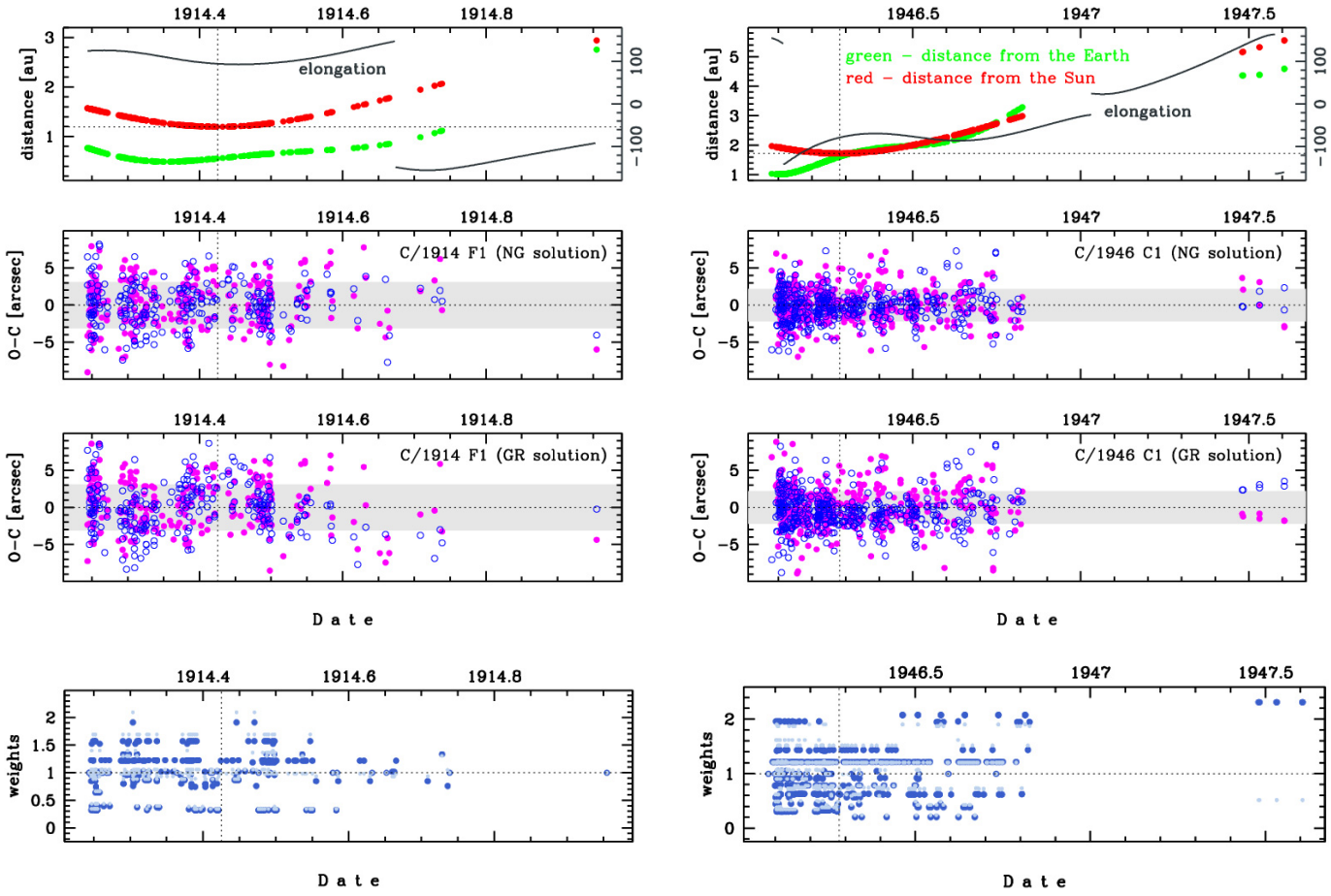

Fig. 2. O–C diagrams for comets C/1914 F1 Kritzinger (*left-hand panels*) and C/1946 C1 Timmers (*right-hand panels*). *Upper panels* show the time distribution of positional observations with corresponding heliocentric (red curve) and geocentric (green curve) distance at which they were taken (left-hand vertical axes). Horizontal dotted lines show the perihelion distance and vertical dotted lines the moment of perihelion passage. Dark grey curves represent the change of the comet's elongation within the observed time intervals (right-hand vertical axes range from −180 to 180 degrees). The second panels from the top present the O–C based on NG solutions, the third panels show O–C based on a pure GR orbit. Residuals in right ascension are shown as magenta dots and in declination as blue open circles. The lowest panels show the comparison between the normalized weights of data between NG solution (dark blue points) and GR solution (light steel-blue points).

NG model assumes that water sublimates from the whole surface of an isothermal cometary nucleus. An asymmetric model of NG acceleration is derived by using $g(r(t-\tau))$ instead of $g(r(t))$ (Yeomans & Chodas 1989; Sitarski 1994). This last model introduces an additional NG parameter τ – the time displacement of the maximum of the $g(r)$ relative to the moment of perihelion passage. We found that only the symmetric model of NG motion was applicable for the comets investigated here.

Using the formalism described above, we found satisfactory NG models for thirteen of the 38 investigated near-parabolic comets. The NG parameters found for all these comets are presented in Table B.2. We noticed some traces of NG effects in the motion of some other comets, but we decided to present here only the NG solutions where we noticed an improved orbit fitting in comparison to a pure gravitational orbit. This improved fitting was measured by three criteria (Królikowska & Dybczyński 2013):

- decrease in rms residual,
- overcoming or reducing the improper trends in O–C time variations,
- increasing the similarity of the O–C distribution to a Gaussian distribution.

Solutions that include the NG effects in the model of motion are highlighted by grey shading in Tables A.1, B.1, C.1, D.1, and E.1. The rms residual for all NG solutions presented here is lower than the GR solutions (Col. (9) of Table C.1). In the following two subsections we discuss some examples that illustrate the improved time variation and statistical distribution of O–C residuals when NG accelerations are included in the comet motion.

4.1. O–C time variations

Two examples of how the NG model of motion improves the O–C vs. time diagram are presented in Fig. 2 for comets C/1914 F1 Kritzinger (0.48 yr data span, $q_{\rm osc}$ = 1.20 AU) and C/1946 C1 Timmers (1.52 yr data span, $q_{\rm osc}$ = 1.72 AU), which have second- and first-class orbits, respectively.

4.1.1. NG solutions for comets of second-class orbits

Comets of second-class orbits need special care during the NG solution because of the relatively large rms residuals. We were surprised to find NG trends in data for five such comets.

Among these five are three comets (C/1906 B1, C/1911 S3 and C/1921 E1) with hyperbolic original, barycentric orbits. We chose C/1914 F1, which has 2a/2b class GR/NG orbits, to visualize the differences between GR and NG solutions in O–C time variations. However, we also discuss in detail the differences between NG and GR solutions for the remaining four comets of second-class orbits.

The O–C time variations for C/1914 F1 are compared in the left-hand part of Fig. 2. One can see wavy trends with time in declination for the purely gravitational solution (blue open dots in the third panel from the top). Additionally, almost all residuals in right ascension and declination from 1914 August 26 to the last observation are negative. Both trends disappear in the NG model of motion (second panel). This improvement in O–C time variations is accompanied by a reduced rms residual from 3.″33 to 3.″12 (see Table C.1). Moreover, the O–C distribution for the NG orbit is perfectly Gaussian with $\chi^2 = 15.9$ for 18 degrees of freedom, while the critical $\chi^2(18, 0.05)$-value associated with the number of degrees of freedom (18) and assumed significance level (0.05) equals 28.9. The purely gravitational orbit gives a poorer fitting to a normal distribution (with $\chi^2 = 24.7$ for 18 degrees of freedom).

Thus, the NG orbit seems to be a more adequate solution for C/1914 F1, although the NG osculating orbit is determined with very poor accuracy (2b class). It yields an original inverse semi-major axis of $(600 \pm 152) \times 10^{-6}$ AU^{-1}, that is, far beyond the Oort spike, but within 3 sigma combined error, this value is consistent with the $1/a_{\rm ori} = (57 \pm 28) \times 10^{-6}$ AU^{-1} that results from a purely GR solution. In our opinion this NG orbital solution better describes both the actual motion of this comet and our actual knowledge of the orbital elements.

Generally, the NG model of motion (if determinable) is always closer to reality. However, in this model we always need to determine additional parameters together with the orbital elements. Thus, the uncertainties of orbital elements of a NG orbit are usually larger than those of a GR orbit for the same comet. Nevertheless, the NG solution with its larger uncertainties more adequately describes our actual knowledge of the dynamics of an individual comet.

This argument was also an important reason to give NG solutions for two other comets of second-class orbits, C/1911 S3 (0.38 yr data span, $q_{\rm osc} = 0.303$ AU) and C/1937 N1 (0.49 yr data span, $q_{\rm osc} = 0.86$ AU). In both cases, the data interval is about as short as for C/1914 F1. Additionally, the data structure is similar for all three comets.

In the C/1911 S3 data, the gap in observations toward the end of data goes from 1911 October 29 to 1912 Jan. 28 with five more observations from January 29 to February 17 taken by C.D. Perrine at Cordoba (National Observatory, Argentina). The eccentricity of the osculating orbit determined by us ($e = 1.000174$ on the basis of 246 residuals) is closer to the value derived originally by Grubissich (1952, $e = 1.000170$ on the basis of 128 measurements) than to that obtained by MSE and given in MW08 ($e = 1.000147$, on the basis of only 66 observations).

For C/1937 N1 a similar lack of data exists from 1937 October 6 to December 29, and the last single measurement was taken on December 30 by J. Bobone also at Cordoba. The importance of the last measurements of data is evident in both cases. We noticed a better fitting of the terminal data in NG solutions for both comets, but with significantly less improvement in overall O–C time variation for C/1937 N1 than for C/1914 F1. We conclude that NG effects are visible mainly in the decrease of rms residual (see Col. (9) of Table C.1).

Similar to the C/1914 F1 case, NG solutions of C/1911 S3 and C/1937 N1 result in significant shifts of $1/a_{\rm ori}$ to more positive values (Sect. 5).

Two more comets with determinable NG effects and second-class orbits are C/1906 B1 and C/1921 E1. Both comets were observed longer than those discussed above and have a gap in observations at the beginning (C/1906 B1, six-month lack of data) or close to the end (C/1921 E1, three-month lack of observations) of data sequences. This data structure causes two prediscovery observations in July 1905 to extend the data period from three to nine months for C/1906 B1. Thus, these two prediscovery observations are crucial for determining the NG effects in the motion of this comet. In the second case, the situation is slightly different because at the end of data we have a sequence of four observations from 1921 October 2 to 1921 November 26. All of them were taken by W.H.W. Baade, who was the only observer that followed the comet after the three-month gap in data caused by the comet's conjunction with the sun. In the GR solution all residuals are negative in both right ascensions and declination. This trend disappears for the NG orbit.

4.1.2. NG solutions for comets of first-class orbits

Of the eight comets from this group we selected C/1946 C1 for the detailed discussions because it has a characteristic data structure with a large gap at the end of the time sequence of observations (right panel of Fig. 2). In this case, the six measurements taken by H. M. Jeffers using the 36-inch Crossley reflector at Lick Observatory (Mount Hamilton) are crucial for osculating orbit determinations. He photographed the comet in 1947 on June 24–25, July 13, and August 9. These observations extended the observation interval by almost ten months. In the third right-side panel from the top, all six measurements show a trend towards increasingly negative residuals in right ascension and increasingly positive residuals in declination for a purely GR solution. In this case the rms residual decreases from 2.″53 (GR solution) to 2.″17 (NG solution, see Table C.1).

The bottom panels of Fig. 2 show a close similarity in normalized weights of data between the NG solution (dark blue points) and the GR solution (light steel-blue points) for the entire data interval (C/1914 F1) or almost all measurements (C/1946 C1). This merits a brief comment. Normalized weights obtained in the GR model for the measurements taken at Mount Hamilton (about 0.5) suggest that these data are of lower accuracy than the average subset of measurements in this data set, while assuming a NG model of motion, we derive that these data fit the model best of all groups of measurements taken for this comet. This is an additional indication that the NG model better describes the actual motion of C/1946 C1.

This behaviour of weights is rather typical for all comets investigated here. However, sometimes there are even trends in weights for GR models in contrast to NG models (see Sect. 4.2).

4.2. O–C distributions

Two other examples provide a comparison of O–C distributions between three types of models: (i) the GR model determined using selected data; (ii) the GR model based on selected and weighted data; and (iii) the NG model also based on selected and weighted data. Observations were always individually selected and/or weighted during each process of orbit determination for each model (see bottom panels in Fig. 2). The upper

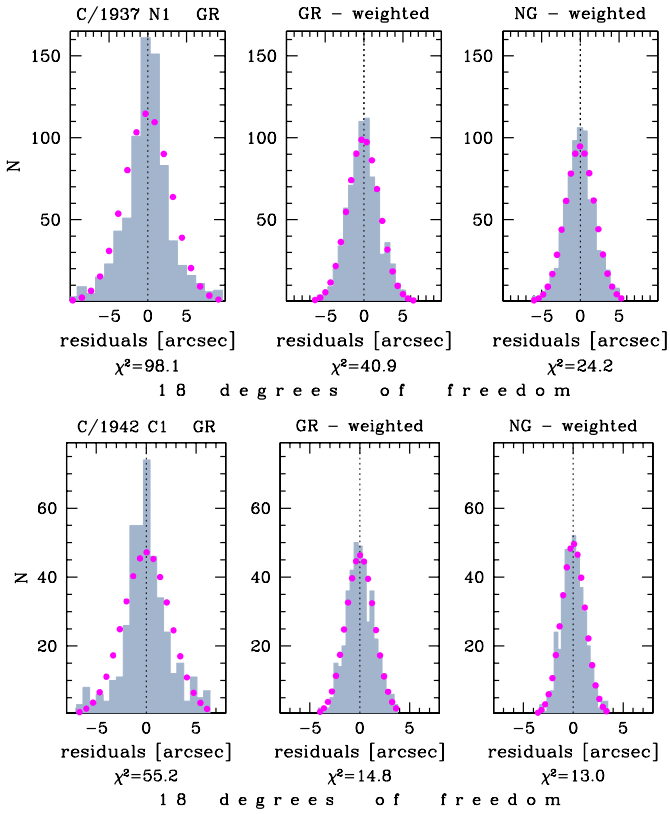

Fig. 3. O–C residual distributions taken for orbit determination for comets C/1937 N1 Finsler (*upper panels*, second-class GR/NG orbits) and C/1942 C1 Whipple-Bernasconi-Kulin (*lower panels*, first-class GR/NG orbits). For both comets three types of solutions are shown, *from left to right*: pure GR solution based on non-weighted data, pure GR solution based on weighted data, and NG solution derived using weighted data. The best-fitting Gaussian distributions are shown by magenta dots, each chosen to lie exactly in the middle of a histogram bin.

panels of Fig. 3 display the residual distributions for C/1937 N1 Finsler and the lower panels those for C/1942 C1 Whipple-Bernasconi-Kulin (here, we present the combined distributions of the residuals in right ascension and declination since in our weighting procedure we applied the simplifying assumption of equal weight in right ascension and declination for an individual measurement). In both cases, about 8–9% of the residuals are rejected in all three models, while the orbit of C/1937 N1 in MW08 was determined using only about 50 per cent of the data collected in the literature by us, and for C/1942 C1, we have fewer observations than declared in MW08.

The best-fitting normal distribution for the data sets of both comets deviates significantly when all measurements were taken with equal weights. Moreover, the asymmetry of the residual distribution is noteworthy (leftmost distributions in both sets of panels of Fig. 3). The improvement of the fit to a Gaussian distribution is remarkable when we include the weighting procedure in the GR orbit determination in both cases. The goodness of the fits of the derived O–C distributions to Gaussians was measured by the Pearson chi-squared test. Additionally, we calculated the kurtosis (related to the fourth moment of the distribution) and skewness (related to the third moment), and thus controlled whether/how the deviations from the normal distribution decrease when NG effects are included in the model of motion. The values of χ^2-test and the number of degrees of freedom are presented below each histogram in Fig. 3.

As was mentioned before, the critical $\chi^2(18, 0.05)$ value equals 28.9. This means that in for C/1937 N1 both GR solutions give residual distributions inconsistent with a hypothesized normal distribution, while for C/1942 C2 the residual distributions for GR-weighted solution ($\chi^2 = 14.8$) fit a normal distribution very well. For C/1937 N1 the deviation can be interpreted to mainly result from the inadequacy of the GR model. Hence, NG effects may be suspected in the motion of this comet. When these are included in the model, the resulting distribution of residuals gives $\chi^2 = 24.2$, indicating that the residual distribution for the NG model is consistent with a normal distribution at the assumed significance level of 0.05. This is different for C/1942 C1. Already the GR solution based on weighted data gives an excellent fit to a normal distribution, similarly as the NG solution does.

The examples given in Fig. 3 are representative for all comets with determinable NG effects. Thus, in some cases, we do not observe improvements in the fit to a normal distribution between GR and NG models. However, the decrease of rms and O–C time variations indicate that the NG model better represents the data set than the GR solution. Additionally, sometimes we noticed that the weights determined in a GR model try to compensate for trends in residuals by a more of less systematic decrease of weights for measurements at the end of the data interval. In the NG models these trends disappear.

5. Original and future orbits

To derive original and future reciprocal semi-major axes for each comet, we performed dynamical calculations backward and forward in time out to 250 AU from the Sun, that is, to a location where planetary perturbations are completely negligible (Todorovic-Juchniewicz 1981). In the present investigation of dynamical evolution, the numerical calculations for a given object start from a swarm of virtual comets (hereafter VCs) constructed using the osculating orbit (so-called nominal osculating orbit) determined in the respective model shown in Table B.1. For comets with determinable NG effects, we calculated two types of evolution: the pure GR evolution starting from the purely gravitational osculating orbit, and the NG evolution starting from the NG osculating orbit.

Each individual swarm of starting osculating orbits consists of 5 001 VCs including the nominal orbit and is constructed according to the Monte Carlo method proposed by Sitarski (1998), where the entire swarm fulfils the Gaussian statistics of fits to positional data for a given osculating orbit determination. All $1/a$-distributions and the distributions of other orbital elements of the analysed swarm of VCs were still perfectly Gaussian at 250 AU from the Sun.

Hence, we are able to determine the uncertainties of original and future orbital elements, including the reciprocal semi-major axes, by fitting each original/future swarm of VC orbital elements to a Gaussian distribution. These uncertainties of orbital elements are given together with original/future elements in Cols. (3)– (9) of Table D.1/E.1. Additionally, Table C.1 shows differences in original and future values of 1/a between MW08 (Cols. (4) and (6)) and our investigation (Cols. (7)– (8)).

Assuming that orbits listed in MW08 have intrinsic errors (uncertainties) on the same level as ours, we found that our $1/a_{\rm ori}$ for GR orbits are consistent within about combined 3 sigma with those given in MW08 for almost all comets investigated here. This fact is illustrated in Figs. 4 and 5. In both figures our GR solutions for comets of first-class orbits (1a or 1b) are plotted in

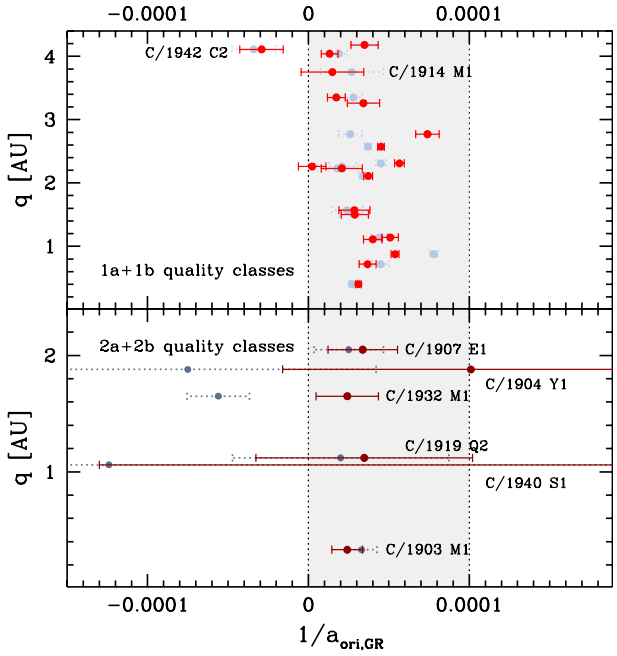

Fig. 4. Comparison between $1/a_{\rm ori,GR}$ (red and dark red points and their error bars) for 25 comets with indeterminable NG effects and values given in MW08 (light and dark steel-blue points), where the uncertainties were assumed to be the same as ours (dotted error bars). The *upper panel* presents comets of first-class orbits, while the *bottom panel* shows six comets having second-class orbits according to the new, more restrictive quality assessment. C/1903 M1, C/1904 Y1, and C/1940 S1 belong to the comets with the shortest intervals of observations among all investigated objects (less than 0.42 yr). On the other hand, three comets with the largest $1/a$-uncertainties among first-class orbits (C/1914 M1, C/1942 C2 and C/1944 K2) were observed for more than 1 yr.

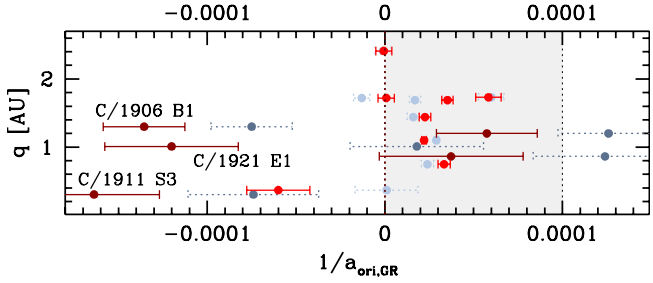

Fig. 5. Same as in Fig. 4 for GR solutions for 13 comets where we determined NG effects (compare also with Fig. 6). Four negative $1/a_{\rm ori,GR}$ belong to comets from left to right: C/1911 S3 (q = 0.303 AU, orbital quality class: 2a/2b, MW08: 2A), C/1906 B1 (q = 1.30 AU, class: 2a, MW08: 1B), C/1921 E1 (q = 1.01 AU, class: 2a, MW08: 1B) and C/1940 R2 (q = 0.368 AU, class: 1b, MW08: 1B). Two more points with large uncertainties of $1/a_{\rm ori,GR}$ represent comets C/1937 N1 (q = 0.863 AU, class: 2a, MW08: 2A) and C/1914 F1 (q = 1.20 AU, class: 2a/2b, MW08: 2A). Our values of the original inverse semi-major axis for C/1946 U1 (q = 2.41 AU) and C/1937 C1 (q = 1.73 AU) are almost the same as in MW08; hence the steel-blue points are invisible.

red, and those of second-class orbits (2a or 2b) in dark red. The $1/a_{\rm ori}$ values in MW08 are shown by light steel-blue points with dotted assumed error bars.

With the classic MSE paper, it became clear that NG effects are important for determining the original inverse semi-major axis for long-period comets. In a series of papers, Królikowska (2001, 2004, 2006) showed that by including the NG accelerations into the model of motion, slightly different osculating

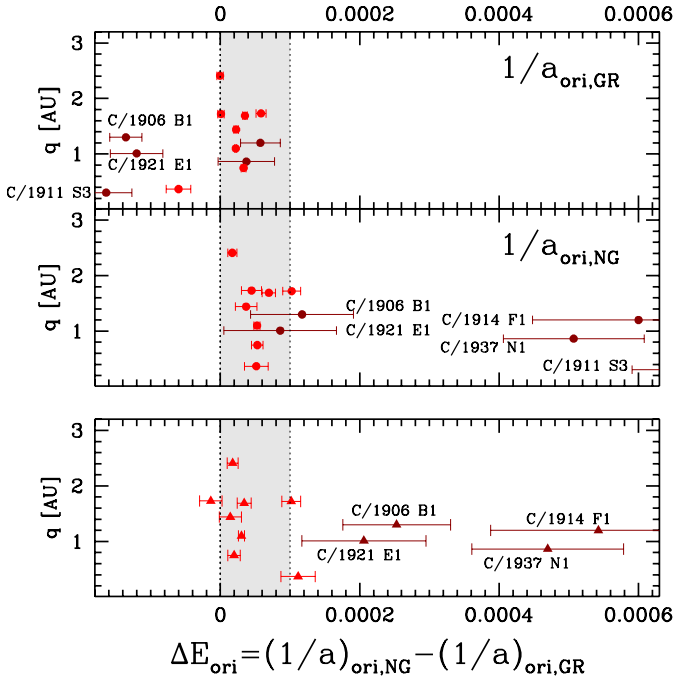

Fig. 6. Shifts of $1/a_{\rm ori}$ caused by the NG acceleration for thirteen comets from the period 1901–1950. The five largest uncertainties of $1/a_{\rm ori,NG}$ (*middle panel*) and $\Delta E_{\rm ori}$ (lowest plot) belong to comets of second-class orbits.

orbits were derived than when assuming purely gravitational motion, and these subtle differences can significantly change the original semi-major axes of these near-parabolic comets. This effect is also clearly visible for comets investigated here. The differences between the reciprocal semi-major axes derived in the NG and GR models of motion are illustrated for 13 comets examined here in Fig. 6 (C/1911 S3 is outside the right border in the lowest panel). In this sample of comets with detectable NG effects there are eight comets with first-class orbits (1a and 1b) and five with second-class orbits. The latter five are recognizable in Fig. 6 by dark red colour and significantly larger uncertainties of $1/a_{\rm ori}$ than the remaining eight comets.

Limiting ourselves to comets with first-class orbits, the change of $1/a_{\rm ori}$ due to incorporating the NG effects causes one of eight comets to be situated exactly on the border line of Oort spike area.

All comets with second-class orbits are significantly shifted towards higher values of $1/a_{\rm ori}$, that is, considerably smaller semi-major axes. However, the uncertainties of the derived $1/a_{\rm ori}$ are very large and preclude any conclusion, except for the conclusion that three second-class objects do not seem to be Oort spike comets. According to the solutions listed in MW08, only two of them (C/1914 F1 and C/1937 N1) are slightly beyond the right border of the Oort spike region (two dark steel-blue points on the right side of Fig. 5). It is interesting to note that our GR solutions yield $1/a_{\rm ori}$ well inside the Oort spike for both these comets (two dark red points in the middle of the figure).

Only one comet, C/1942 C2 (orbit of first class), in the investigated sample has a hyperbolic barycentric original orbit of $1/a_{\rm ori} = (-29.1 \pm 13.5) \times 10^{-6}\,{\rm AU}^{-1}$ (upper panel of Fig. 4). This comet has a perihelion distance larger than 4 AU, and we were only able to determine a GR solution. At the level of 3 sigma, this comet does not have to be a stranger coming from the interstellar space, but it could be a comet of the solar

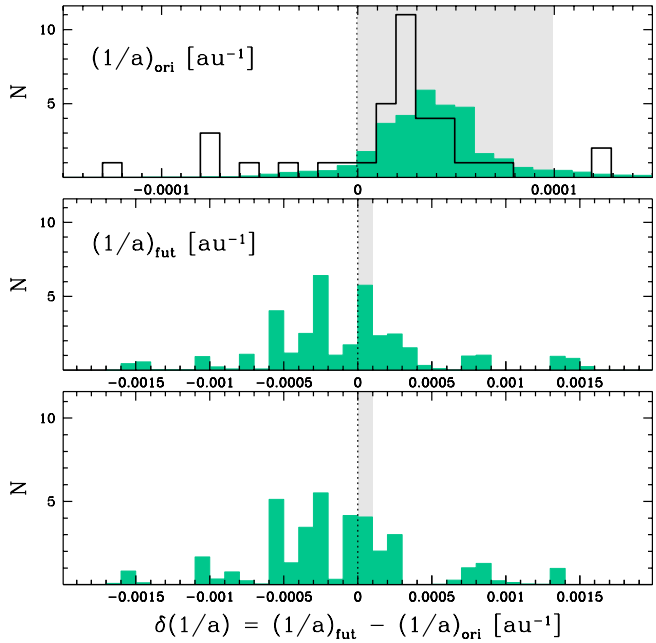

Fig. 7. Distribution of $1/a_{\rm ori}$ (*top panel*), $1/a_{\rm fut}$ (*middle panels*) and $\delta(1/a)$ for considered LPCs. The black histogram given in the top panel represents the distribution taken from MW08. The uncertainties of our $1/a$-determinations were incorporated in these $1/a$-histograms by taking the full cloud of VCs for each comet. Two comets are outside the right border in the upper plot: C/1914 F1 ($1/a_{\rm ori}$ = 600 ± 153, orbit of 2b class) and C/1937 N1 ($1/a_{\rm ori}$ = 507 ± 101, 2a class), both with NG orbits.

system. This comet also has a formally negative value of $1/a_{\rm ori} = -34\times10^{-6}$ AU^{-1} in MW08, very close to our value. Of the seven more comets with negative $1/a_{\rm ori}$ in MW08, only three have orbits of second class (in MW08), and one more case of $1/a_{\rm ori}$ is marginally negative. Four of these hyperbolic comets in MW08 (C/1906 B1, C/1911 S3, C/1946 C1 and C/1946 U1) have determinable NG effects according to our investigations with elliptic original orbits, as shown in the middle panel of Fig. 6. The remaining three have positive $1/a_{\rm ori}$ in our GR model of motion (C/1904 Y1, C/1932 M1, and C/1940 S1, see Table C.1).

Figure 6 shows the $1/a_{\rm ori}$-shifts caused by incorporating the NG effects in the model of motion. The five largest $1/a_{\rm ori}$-shifts are observed for comets of second-class orbits. However, the uncertainties of the $1/a_{\rm ori}$ determination are also large in all these cases. The goodness of NG model fit to the positional data compared to the GR model is discussed in detail in Sect. 4.1.1 for all these objects. The largest $1/a_{\rm ori}$-shift is observed for C/1911 S3 (far outside the right border of Fig. 6), where a pure GR solution gives a hyperbolic original orbit both in the present investigation and in MW08.

The distributions of $1/a_{\rm ori}$ and $1/a_{\rm fut}$ are presented in Fig. 7 in the upper and middle panels. The middle panel and Table C.1 show that 19 comets (50%) are escaping from the solar system on hyperbolic orbits, and one more, C/1914 M1, has a marginally bound future barycentric orbit.

In the upper panel of Fig. 7 we compare our results for the best models of motion (turquoise distribution) with those taken from MW08 (black histogram). The difference between distributions of $1/a_{\rm ori}$ is striking. The distribution resulting from our investigation is wider and shifted towards higher values of $1/a_{\rm ori}$. This difference results from $1/a_{\rm ori}$-shifts caused by NG effects derived for 13 comets (1/3 of the sample) and because uncertainties of $1/a_{\rm ori}$ were incorporated in our distribution. For

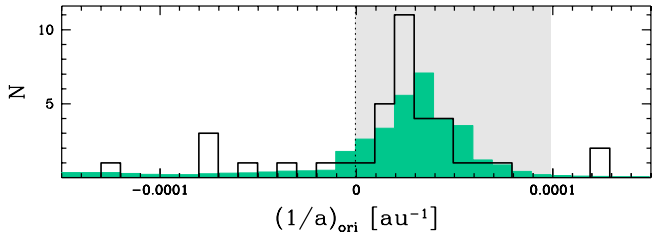

Fig. 8. Same as in the top panel of Fig. 7 when only pure GR solutions are taken into consideration.

comparison, Fig. 8 displays the $1/a_{\rm ori}$-distribution for our GR solutions alone. Thus, both plots are based on 38 swarms × 5001 = 190 038 VCs, where each swarm of 5001 VCs fits to the respective data set well.

The largest uncertainties of $1/a_{\rm ori}$ (larger than 50 in units of 10^{-6} AU^{-1}) belong to comets C/1940 S1 Okabayashi-Honda ($1/a_{\rm ori}$ = 297 ± 427, NG orbit of 2b class), C/1911 S3 Beljawsky ($1/a_{\rm ori}$ = 796 ± 205), NG orbit, 2b class), C/1914 F1 Kritzinger ($1/a_{\rm ori}$ = 600 ± 153, NG orbit, 2b class), C/1904 Y1 Giacobini ($1/a_{\rm ori}$ = 101 ± 117, GR orbit, 2b class), C/1937 N1 Finsler ($1/a_{\rm ori}$ = 507 ± 101, NG orbit, 2a class), C/1921 E1 Reid ($1/a_{\rm ori}$ = 85.9 ± 80.8, NG orbit, 2a class), and C/1919 Q2 Metcalf ($1/a_{\rm ori}$ = 34.7 ± 67.3, GR orbit, 2a class); see also Figs. 4 and 6. The first, C/1940 S1, forms an almost constant and negligible background for the 1/a-distribution. The next three comets (C/1911 S3, C/1914 F1 and C/1937 N1) have $1/a_{\rm ori}$ formally far outside the right border of the Oort spike, within 3–4σ error barely reaching the right side of the Oort spike, and practically do not contribute to the Oort spike distribution either. The distribution of $1/a_{\rm ori}$ of the remaining three comets (C/1904 Y1, C/1921 E1 and C/1919 Q2) are scattered throughout the entire Oort spike according to their individual $1/a$-Gaussians. Almost all remaining investigated comets have uncertainties of their $1/a_{\rm ori}$ comparable to the width of a single bin in Fig. 7. Thus, it is obvious that $1/a_{\rm ori}$-errors should be taken into account for Oort spike construction, as was done in Figs. 7, 8.

The shape of Oort spike distribution based on 157 near-parabolic comets is presented in the upper panel of Fig. 9, where 119 comets analysed by Królikowska (2014) were included. The maximum of $1/a_{\rm ori}$ is broad and extends between 0.000010 and 0.000065 AU^{-1}. This $1/a_{\rm ori}$-distribution seems to have a local minimum somewhere between 0.000025 and 0.000035 AU^{-1} (spans over at least two bins). It is important to stress here that histograms based on twice wider bins give different shapes depending on how we distributed these wider bins (zero point in the middle of the bin or on its edge).

The lower panel of Fig. 9 shows the distribution of the future reciprocals of semi-major axes. About 50% of these comets leave the solar system on hyperbolic, barycentric orbits, and 13% of the future semi-major axes are still inside the Oort spike. Recent simulations performed by Fouchard et al. (2013) give very similar values, although a little lower. The narrow peak in the range $|1/a_{\rm fut}| < 0.000100$ AU^{-1} is striking and includes about 30% of the entire sample. This means that a significant number of these actual comets suffers small planetary perturbations during the passage through the planetary zone.

6. Summary

The four main features that distinguish this catalogue of orbits of one-apparition comets discovered in the early twentieth century

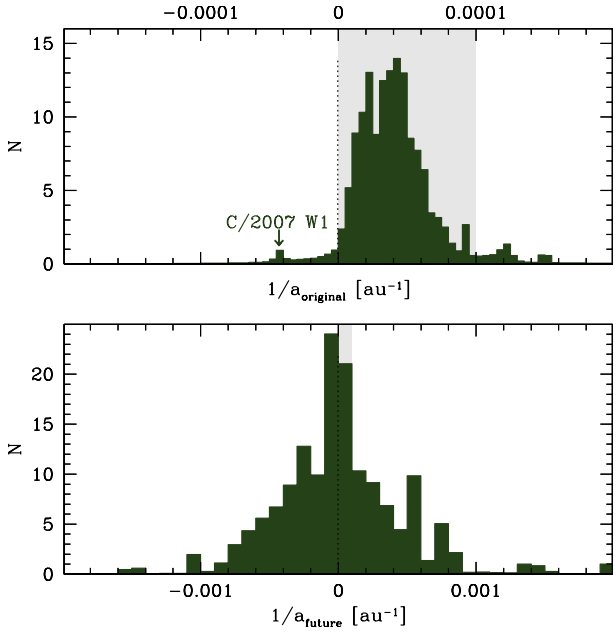

Fig. 9. Same as in the *top and middle panels* of Fig. 7, but including 119 comets taken from Królikowska (2014). Both distributions are composed of 157 individual normalized $1/a$-distributions, each resulting from the dynamical calculations of 5001 VCs.

from other catalogues of orbits of similarly old objects are the following:

1. Old cometary positional observations require very careful analysis. For the purpose of this new catalogue, great emphasis has been placed on collecting sets of observations as complete as possible for the investigated comets. Moreover, for many observations comet-minus-star measurements were also available. This type of data was particularly valuable as the most original measurement of comet positions and has allowed us to recalculate new positions of comets using the PPM star catalogue.
2. Old cometary observations were prepared by observers usually as apparent positions in right ascension and declination or as reduced positions for the epoch of the beginning of the year of a given observation. This was a huge advantage of these data, because it allowed us to uniformly take into account all necessary corrections associated with the data reduction to the standard epoch.
3. Osculating orbits of one-apparition comets discovered more than sixty years ago have formerly been determined with very different numerical methods and assumptions on the model of the solar system, including the number of planets taken into account. This new catalogue changes this situation. We offer a new catalogue of cometary orbits derived using completely homogeneous methods of data treatment, accurate methods of numerical integration, and a modern solar system model.
4. The osculating, original, and future sets of orbits are presented for each catalogue comet. For a comet with detectable NG effects, we give both types of orbit: purely gravitational and non-gravitational. We conclude, however, that all thirteen NG orbital solutions given in the catalogue better represent the actual motions of the investigated comets. Surprisingly, NG effects were detectable in data for five comets of second-class orbits. Among these five are three comets (C/1906 B1, C/1911 S3, C/1921 E1) with hyperbolic original, barycentric GR orbits.

Acknowledgements. This publication is dedicated to the memory of Maciej Bielicki (1906–1988), one of the initiators of this catalogue of one-apparition comets. The orbits were calculated using the numerical orbital package developed by Grzegorz Sitarski and the Solar System Dynamics and Planetology Group at SRC PAS. Special thanks to everyone who, many years ago, participated in the data collection from the literature and in the very preliminary analysis of these observations, among others, Wanda Borodziewicz and Tomasz Chlebowski.

References

Bielicki, M. 1972, in The Motion, Evolution of Orbits, and Origin of Comets, eds. G. A. Chebotarev, E. I. Kazimirchak-Polonskaia, & B. G. Marsden, IAU Symp., 45, 112
Bielicki, M., & Sitarski, G. 1991, Acta Astron., 41, 309
Bielicki, M., & Ziołkowski, K. 1976, Acta Astron., 26, 371
Fouchard, M., Rickman, H., Froeschlé, Ch., & Valsecchi, G. B. 2013, Icarus, 222, 20
Gabryszewski, R. 1997, P&SS, 45, 1653
Grubissich, C. 1952, Mem. Soc. Astron. It., 22, 251
IAU Minor Planet Center, 2013, MPC Database Search, URL http://www.minorplanetcenter.net/db_search/
Królikowska, M. 2001, A&A, 376, 316
Królikowska, M. 2004, A&A, 427, 1117
Królikowska, M. 2006, Acta Astron., 56, 385
Królikowska, M. 2014, A&A, 567, A126
Królikowska, M., & Dybczyński, P. A. 2010, MNRAS, 404, 1886
Królikowska, M., & Dybczyński, P. A. 2013, MNRAS, 435, 440
Królikowska, M., Sitarski, G., & Sołtan, A. M. 2009, MNRAS, 399, 1964
Kronk, G. W. 2008, Cometography. A Catalog of Comets, 3, 1900
Marsden, B. G., & Williams, G. V. 2008, Catalogue of Cometary Orbits 17th Ed. (Cambridge, Mass.: Smithsonian Astrophysical Observatory)
Marsden, B. G., Sekanina, Z., & Yeomans, D. K. 1973, AJ, 78, 211
Marsden, B. G., Sekanina, Z., & Everhart, E. 1978, AJ, 83, 64
Rickman, H., Sitarski, G., & Todorovic-Juchniewicz, B. 1987, A&A, 188, 206
Sitarski, G. 1972, in The Motion, Evolution of Orbits, and Origin of Comets, eds. G. A. Chebotarev, E. I. Kazimirchak-Polonskaia, & B. G. Marsden, IAU Symp., 45, 107
Sitarski, G. 1979a, in Dynamics of the Solar System (Dordrecht: D. Reidel Publishing Co), IAU Symp., 81, 289
Sitarski, G. 1979b, Acta Astron., 29, 401
Sitarski, G. 1984, Acta Astron., 34, 53
Sitarski, G. 1989, Acta Astron., 39, 345
Sitarski, G. 1992, AJ, 104, 1226
Sitarski, G. 1994, Acta Astron., 44, 91
Sitarski, G. 1998, Acta Astron., 48, 547
Sitarski, G. 2002, Acta Astron., 52, 471
Standish, E. M. 1998, JPL Planetary and Lunar Ephemerides, DE405/LE405, Tech. Rep. IOM 312.F–98–048
Todorovic-Juchniewicz, B. 1981, Acta Astron., 31, 192
Williams, G. V. 2005, Minor Planet Circulars, 54698, 6
Yeomans, D. K., & Chodas, P. W. 1989, AJ, 98, 1083

Appendix A: Collected observational data and data processing

Table A.1. Collected observational material for the sample of 38 LPCs discovered during 1901–1950 (Cols. (4)–(7)).

			Observational material				MW 08	
Comet name	q_{osc}	T	Observational arc dates	No. of obs	Data arc span	Heliocentric distance span	Observational arc dates	No. of obs
	[AU]	[yyyymmdd]	[yyyymmdd–yyyymmdd]		[yr]	[AU]	[yyyymmdd–yyyymmdd]	
(1)	(2)	(3)	(4)	(5)	(6)	(7)	(8)	(9)
C/1902 R1	0.401	19021124	19020901–19030331	1491	0.58	1.79–2.44	19020901–19030331	1000
C/1902 X1	2.77	19030323	19021202–19030627	735	0.57	3.00–2.94	19021204–19030624	191
C/1903 M1	0.330	19030828	19030629–19031023	653	0.36	1.52–1.36	19030622–19031023	231
C/1904 Y1	1.88	19041103	19041218–19050502 post	164	0.37	1.96–2.86	19041218–19050502	48
C/1906 B1	1.30	19051222	19050723–19060425 post+	267	0.76	2.50–2.18	19050723–19060424	186*
C/1906 E1	3.35	19051018	19040110–19070704** post+	462	3.48	6.53–6.38	19040110–19070704	500
C/1907 E1	2.05	19070319	19070309–19080226	178	0.97	2.05–4.29	19070309–19080226	67
C/1911 S3	0.303	19111010	19110929–19120217[1]	162	0.38	0.46–2.55	19110930–19120217	66
C/1912 R1	0.716	19121005	19120911–19130526[2]	935	0.71	0.86–3.59	19120910–19130526	170
C/1913 Y1	1.10	19141026	19131218–19150907[3]	1006	1.72	4.24–4.26	19131218–19150907	339
C/1914 F1	1.20	19140604	19140330–19141214	285	0.48	1.57–2.94	19140330–19141214	62
C/1914 M1	3.75	19140730	19140624–19150810[4]	70	1.13	3.76–4.96	19140628–19150715	39
C/1916 G1	1.69	19170617	19160407–19180129	471	1.81	5.16–5.74	19160404–19180129	186
C/1919 Q2	1.12	19191207	19190825–19200203	276	0.44	1.95–1.75	19190825–19200203	87
C/1921 E1	1.01	19210510	19210315–19211126	568	0.70	1.74–2.25	19210315–19211126	146
C/1922 U1	2.26	19221026	19221022–19240128 post+	482	1.27	2.26–5.22	19221022–19240128	185
C/1925 F1	4.18	19250906	19250323–19270304[5]	262	1.95	4.41–6.07	19250323–19270304	59
C/1925 G1	1.11	19250401	19250405–19260502[6] post	598	1.07	1.11–5.15	19250405–19260502	201
C/1925 W1	1.57	19251002	19251117–19260610[7] post	342	0.56	1.57–3.47	19251117–19260531	129
C/1932 M1	1.65	19320924	19320621–19330120[8]	187	0.58	2.06–2.25	19320621–19321230	48
C/1932 M2	2.31	19320921	19310814–19340719	328	2.93	4.78–6.83	19310814–19340719	161
C/1935 Q1	4.04	19360511	19350703–19371112[9]	131	2.30	4.83–6.06	19350703–19371110	107
C/1937 C1	1.73	19370620	19370204–19371028	417	0.72	2.44–2.40	19370204–19371028	136
C/1937 N1	0.863	19370815	19370704–19371230	413	0.49	1.14–2.36	19370704–19371230	212
C/1940 R2	0.368	19410116	19400825–19410401***	370		2.71–1.67	19400919–19410617	189
C/1940 S1	1.06	19400815	19401004–19410103[10] post	36	0.25	1.34–2.37	19401004–19410102	19
C/1941 K1	0.875	19410903	19410604–19420218	461	0.71	1.76–2.74	19410604–19420218	318
C/1942 C1	1.44	19420430	19411228–19430108	224	1.03	2.22–3.51	19411228–19430108	228
C/1942 C2	4.11	19420927	19420212–19430311[11]	47	1.07	4.53–4.35	19420212–19430309	35
C/1944 K2	2.23	19440717	19440601–19450811	36	1.19	2.29–4.66	19440601–19450811	25
C/1946 C1	1.72	19460413	19460129–19470809[12]	485	1.52	1.97–5.56	19460202–19470809	183
C/1946 P1	1.14	19461026	19460813–19481123[13]	144	2.28	1.62–8.17	19460816–19481123	101
C/1946 U1	2.41	19470207	19461102–19481002	141	1.92	2.64–6.32	19461102–19481002	97

Notes. The sample includes all comets that in MW08 have $1/a_{ori} < 130 \times 10^{-6}$ AU^{-1} and orbits of first- or second-class. Columns (2)–(4) show the osculating perihelion distance, perihelion time, and interval of collected data. The data distribution relative to perihelion passage is shown by additional descriptions: "post" in Col. (4) when all observations were taken after perihelion passage, and "post+" when the number of data taken after perihelion passage dominate. Columns (8)–(9) describe the positional data that formed the basis for determining the orbits presented in MW08. Comets with detectable NG effects are indicated here by rows in light grey shading (see also Table C.1). Notes to cases where we found in literature observations outside the data interval given in MW08 (in Col. (8) of this table): [(1)] One observation of poor quality was taken on 1911 September 29. Although a hundred times less weight in comparison to good-quality observations was applied, this measurement was rejected in the selecting and weighting. [(2)] One observation was taken on 1912 May 09, two in 1912 September 09, but all three were rejected as incorrect; a single observation from 1912 September 10 was also rejected. [(3)] Three observations taken on 1913 October 25, 26, and 31 are outliers. [(4)] One observation taken on 1914 June 24 (well fitted in right ascension and declination) and two observations taken on 1915 August 10 (only in declination) were also used here to determine the orbit. [(5)] Two observations were taken on 1925 March 22, but were rejected as outliers. [(6)] One observation was taken on 1925 April 05 and was included in the orbit determination only in right ascension. [(7)] Two observations were taken on 1926 June 09 and 10 and were included in the orbit determination only in right ascension and declination, respectively. [(8)] One observation taken on 1933 January 20 was included in the orbit determination in declination. [(9)] One observation taken on 1937 November 12 was included in declination in the orbit determination. [(10)] Three observations were taken on 1941 January 03 – these were included in the orbit determination only in right ascension. [(11)] Two observations were taken on 1943 March 11 and were included. [(12)] One observation taken on 1946 January 29 was included. [(13)] Two observations were taken on 1946 August 13; the first was included only in declination, and the second in both coordinates. Other notes [(*)] This is the unique case where a large set of observations is available at IAU Minor Planet Center Database. There are 239 positional observations, two of which are prediscovery observations found by Gary W. Kronk; they extend the data interval by about six months (see also Sect. 2). [(**)] Before perihelion only two observations were taken on 1904 January 10 and 1905 January 15. [(***)] Our data interval is significantly shorter than in MW08. Data after 1941 April 01 are needed.

Table A.1. continued.

Comet name	q_{osc}	T	Observational material: Observational arc dates	No of obs	Data arc span	Heliocentric distance span	MW 08: Observational arc dates	No of obs
	[AU]	[yyyymmdd]	[yyyymmdd–yyyymmdd]		[yr]	[AU]	[yyyymmdd–yyyymmdd]	
(1)	(2)	(3)	(4)	(5)	(6)	(7)	(8)	(9)
C/1947 S1	0.748	19480216	19470928–19490206	325	1.36	2.45–4.89	19470928–19490206	123
C/1947 Y1	1.50	19480216	19480118–19481130	124	0.87	1.59–3.85	19480118–19481130	78
C/1948 E1	2.11	19480515	19480313–19500209	247	1.91	2.36–6.65	19480313–19500209	95
C/1948 T1	3.26	19470904	19481007–19500817 post	26	1.86	4.89–9.38	19481007–19500817	26
C/1950 K1	2.57	19510115	19500527–19530119	254	2.65	3.53–7.26	19500527–19530119	38

Table A.2. Collected (➹-★) observations ((comet-star) positions in right ascension and declination).

Comet	Number of ➹-★ obs.	Number of recalculated ➹ positions	Per cent of recalculated observations	Preliminary gravitational solution: before PPM rms [″]	before PPM No. of residuals	after PPM rms [″]	after PPM No. of residuals
(1)	(2)	(3)	(4)	(5)	(6)	(7)	(8)
C/1902 R1	1175	753	51	3.76	2454	3.53	2472
C/1902 X1	606	436	59	3.48	1290	3.37	1301
C/1903 M1	430	379	65	4.39	920	3.76	920
C/1904 Y1	150	132	80	3.32	300	3.26	301
C/1906 B1	226	135	51	4.45	456	3.77	450
C/1906 E1	369	315	68	2.45	775	2.58	806
C/1907 E1	157	129	72	4.14	304	2.82	292
C/1911 S3	137	86	63	3.83	243	3.27	261
C/1912 R1	864	726	77	3.84	1635	2.91	1646
C/1913 Y1	947	788	78	3.33	1773	2.70	1798
C/1914 F1	266	229	92	4.10	496	3.88	500
C/1914 M1	47	29	41	2.83	122	2.41	118
C/1916 G1	375	291	62	3.49	760	3.14	836➹
C/1919 Q2	247	208	75	3.38	488	2.58	498
C/1921 E1	498	392	69	4.64	827	4.49	916➹
C/1922 U1	409	276	57	2.62	738	2.57	823➹
C/1925 F1	193	157	59	4.48	449	4.34	472
C/1925 G1	409	366	61	4.89	946	4.71	968
C/1925 W1	246	201	59	2.92	541	2.39	564
C/1932 M1	111	90	48	3.52	314	2.89	316
C/1932 M2	165	96	29	2.13	521	2.13	536
C/1935 Q1	16	4	3	1.63	248	1.62	248
C/1937 C1	220	187	45	4.42	745	3.49	729
C/1937 N1	170	153	37	3.69	733	3.01	745
C/1940 R2	127	113	31	2.33	612	2.19	605
C/1940 S1	5	2	6	5.11	65	5.10	65
C/1941 K1	111	93	20	3.09	769	3.26	778
C/1942 C1	39	38	17	2.41	414	2.41	414
C/1942 C2	0	0	0	1.65	88	1.65	88
C/1944 K2	0	0	0	1.58	56	1.58	56
C/1946 C1	78	54	11	2.71	828	2.71	828
C/1946 P1	8	5	3	1.13	254	1.13	254
C/1946 U1	33	20	14	1.88	252	1.88	254
C/1947 S1	64	59	18	4.62	551	4.32	553
C/1947 Y1	4	4	3	1.44	198	1.44	198
C/1948 E1	26	23	9	2.44	400	2.31	401
C/1948 T1	0	0	0	0.94	52	0.94	52
C/1950 K1	0	0	0	1.28	466	1.28	466

Notes. Column (3) shows the number of recalculated (➹-★) positions using the PPM catalogue, their percentage in comparison to the entire data set collected here (see Col. (5) of Table A.1) is given in Col. (4). The rms and number of residuals taken for preliminary solution are given in Cols. (5)–(6) – before position recalculations based on PPM catalogue, and in Cols. (7)–(8) – after this recalculation. In some cases only (➹-★) data were published – where a significant number of these observations were successfully processed using the PPM star catalogue are marked by ➹ in Col. (8).

Appendix B: Osculating orbital elements (heliocentric)

Table B.1. Orbital elements of osculating heliocentric orbits for all models described in Table C.1.

Comet	Epoch	T	q	e	ω	Ω	i	$1/a_{\rm osc}$
	[yyyymmdd]	[yyyymmdd.dddddd]	[AU]		[°]	[°]	[°]	[10^{-6} AU^{-1}]
(1)	(2)	(3)	(4)	(5)	(6)	(7)	(8)	(9)
C/1902 R1	19021127	19021124.356684	0.40107241	0.99996675	152.983569	50.740193	156.354721	82.897510
		±.000025	±.00000033	±.00000068	±.000085	±.000087	±.000036	±1.714706
C/1902 X1	19030327	19030323.974159	2.77348499	1.00047034	5.830937	118.810872	43.894598	−169.586058
		±.002541	±.00001328	±.00001976	±.000781	±.000085	±.000258	±7.124391
C/1903 M1	19030903	19030828.108377	0.33018087	1.00040917	127.251980	294.909653	85.015231	−1239.232832
		±.000058	±.00000150	±.00000310	±.000260	±.000054	±.000197	±9.400340
C/1904 Y1	19041116	19041103.774111	1.88176420	1.00034373	40.723034	219.786197	99.600058	−182.662119
		±.013312	±.00010009	±.00022266	±.006760	±.000583	±.000577	±118.316762
C/1906 B1	19051221	19051222.834099	1.29656822	1.00118940	89.875094	287.700661	126.443151	−917.341741
		±.000635	±.00000329	±.00002875	±.000333	±.000299	±.000191	±22.172663
	19051221	19051222.827139	1.29649411	1.00071452	89.873443	287.702585	126.443226	−551.119344
		±.001939	±.00001882	±.00012808	±.000523	±.000592	±.000188	±98.785605
C/1906 E1	19051002	19051018.260509	3.33984993	1.00154602	158.599798	343.621657	4.282129	−462.902333
		±.001894	±.00001427	±.00001830	±.000814	±.000729	±.000190	±5.480122
C/1907 E1	19070309	19070319.606941	2.05167901	1.00099244	317.118563	98.484125	141.659654	−483.718771
		±.001690	±.00001611	±.00004395	±.000810	±.000214	±.000193	±21.419803
C/1911 S3	19111011	19111010.764058	0.30342194	1.00017379	71.712390	89.896351	96.463409	−572.782721
		±.000076	±.00000078	±.00001128	±.000390	±.000423	±.000556	±37.169996
	19111011	19111010.764561	0.30341412	0.99988293	71.714197	89.898109	96.469009	385.827118
		±.000128	±.00000178	±.00006089	±.000508	±.000531	±.001332	±200.696777
C/1912 R1	19121005	19121005.453192	0.71607473	1.00045667	25.621533	298.246936	79.809959	−637.746537
		±.000053	±.00000084	±.00000377	±.000108	±.000110	±.000085	±5.267842
C/1913 Y1	19141104	19141026.767056	1.10445641	1.00016199	97.467346	60.396107	68.038294	−146.670259
		±.000062	±.00000079	±.00000143	±.000028	±.000024	±.000042	±1.291169
	19141104	19141026.767012	1.10444242	1.00009618	97.467000	60.396112	68.038602	−87.082819
		±.000062	±.00000218	±.00000906	±.000059	±.000023	±.000059	±8.203185
C/1914 F1	19140528	19140604.693158	1.19853665	1.00018867	72.224168	200.117415	23.914811	−157.414076
		±.000256	±.00000529	±.00003381	±.000277	±.000322	±.000339	±28.212597
	19140528	19140604.695930	1.19844515	0.99971941	72.225088	200.114528	23.909795	234.127010
		±.000549	±.00002359	±.00012683	±.000443	±.000812	±.001379	±105.833235
C/1914 M1	19140816	19140730.491036	3.74680509	1.00325348	14.000020	271.513791	71.041017	−868.335053
		±.010771	±.00006838	±.00009295	±.002102	±.000168	±.000427	±24.783913
C/1916 G1	19170621	19170617.074175	1.68644587	0.99937443	120.621838	184.457271	25.659093	370.940610
		±.000244	±.00000103	±.00000541	±.000141	±.000054	±.000045	±3.207311
	19170621	19170617.074377	1.68642132	0.99932117	120.621627	184.457166	25.658821	402.529745
		±.000274	±.00000382	±.00000954	±.000182	±.000054	±.000063	±5.658616
C/1919 Q2	19191118	19191207.809648	1.11527223	1.00020566	185.753567	122.098062	46.381870	−184.402616
		±.002096	±.00002732	±.00007480	±.002470	±.000560	±.000174	±67.069931
C/1921 E1	19210421	19210510.449383	1.00845704	1.00049609	64.491010	269.440232	132.187612	−491.931566
		±.000308	±.00000145	±.00003777	±.000236	±.000293	±.000113	±37.457531
	19210421	19210510.453240	1.00843659	1.00018145	64.493716	269.438264	132.188366	−179.930464
		±.000810	±.00000434	±.00007412	±.000563	±.000509	±.000185	±73.500349
C/1922 U1	19221102	19221026.532142	2.25878685	1.00079818	118.298884	221.578280	51.456548	−353.365654
		±.001333	±.00000759	±.00001927	±.000483	±.000054	±.000036	±8.530040
C/1925 F1	19250907	19250906.941564	4.18078079	1.00243417	205.759883	358.539358	146.713185	−582.227554
		±.003963	±.00002336	±.00003527	±.000570	±.000095	±.000143	±8.429946
C/1925 G1	19250331	19250401.506580	1.10948315	1.00060414	36.181542	319.109303	100.022632	−544.519568
		±.000240	±.00000309	±.00000642	±.000283	±.000059	±.000080	±5.784550
C/1925 W1	19251017	19251002.973357	1.56621518	1.00037453	106.398480	335.612555	49.329746	−239.133330
		±.000325	±.00001487	±.00001486	±.000589	±.000042	±.000404	±9.487854
C/1932 M1	19320910	19320924.551075	1.64736493	1.00046840	69.787385	246.090506	78.388394	−284.333505
		±.000982	±.00001195	±.00003229	±.000647	±.000230	±.000200	±19.598751
C/1932 M2	19320910	19320921.074056	2.31356998	1.00140517	329.693866	216.093463	124.988856	−607.359409
		±.000474	±.00000273	±.00000708	±.000143	±.000057	±.000050	±3.060104
C/1935 Q1	19360422	19360511.635659	4.04341779	1.00206616	44.895725	300.561472	66.112186	−510.993085
		±.001683	±.00000969	±.00002076	±.000252	±.000059	±.000052	±5.131166
C/1937 C1	19370706	19370620.063073	1.73378655	1.00014288	107.734884	128.608042	41.551513	−82.409381
		±.000498	±.00000401	±.00001263	±.000305	±.000110	±.000084	±7.285233

Notes. The successive columns signify (1) – comet designation; (2) – epoch, that is, osculation date; (3) – perihelion time [TT]; (4) – perihelion distance; (5) – eccentricity; (6) – argument of perihelion (in degrees), equinox 2000.0; (7) – longitude of the ascending node (in degrees), equinox 2000.0; (8) – inclination (in degrees), equinox 2000.0; (9) – reciprocal semi-major axis in units of 10^{-6} AU^{-1}. Osculating orbits determined using the NG model of motion are indicated by light grey shading.

Table B.1. continued.

Comet	Epoch	T	q	e	ω	Ω	i	$1/a_{\rm osc}$
	[yyyymmdd]	[yyyymmdd.dddddd]	[AU]		[°]	[°]	[°]	[10^{-6} AU^{-1}]
(1)	(2)	(3)	(4)	(5)	(6)	(7)	(8)	(9)
	19370706	19370620.061675	1.73378562	1.00014873	107.734189	128.607821	41.551548	−85.786161
		±.000746	±.00000410	±.00001307	±.000445	±.000150	±.000089	±7.541101
C/1937 N1	19370815	19370815.665333	0.86274422	1.00005979	114.835849	59.420445	146.415278	−69.304214
		±.000189	±.00000040	±.00003586	±.000396	±.000220	±.000197	±41.563567
	19370815	19370815.666463	0.86274100	0.99976776	114.837745	59.421272	146.416972	269.188447
		±.000525	±.00000111	±.00010937	±.001203	±.000665	±.000529	±126.765790
C/1940 R2	19410106	19410116.233869	0.36774076	1.00050751	199.568992	296.590441	49.894827	−1380.069563
		±.000068	±.00000272	±.00000650	±.000117	±.000141	±.000173	±17.681186
	19410106	19410116.234772	0.36774724	1.00040431	199.570995	296.590817	49.893846	−1099.416086
		±.000092	±.00000232	±.00001067	±.000226	±.000180	±.000157	±29.027267
C/1940 S1	19400730	19400815.741520	1.06134353	1.00101170	329.641162	128.060306	133.112612	−953.224013
		±.018720	±.00042312	±.00044419	0.036347	±.006071	±.001116	±418.312774
C/1941 K1	19410903	19410903.184122	0.87479022	1.00026410	85.321879	257.559607	94.517037	−301.899679
		±.000051	±.00000031	±.00000216	±.000038	±.000024	±.000106	±2.473802
C/1942 C1	19420501	19420430.833684	1.44530230	1.00088319	223.415778	340.934552	79.451905	−611.075849
		±.000116	±.00000079	±.00000480	±.000076	±.000017	±.000063	±3.321178
	19420501	19420430.834279	1.44528980	1.00082711	223.416090	340.934741	79.451445	−572.277141
		±.000236	±.00000580	±.00002112	±.000147	±.000065	±.000242	±14.612225
C/1942 C2	19421008	19420927.280025	4.11339144	1.00316671	163.620216	281.038570	172.514474	−769.854598
		±.007703	±.00003196	±.00005609	±.001441	±.000853	±.000124	±13.624279
C/1944 K2	19440601	19440717.611796	2.22594125	1.00205322	336.973475	203.500207	95.004881	−922.405433
		±.001868	±.00001342	±.00002843	±.000686	±.000194	±.000159	±12.770486
C/1946 C1	19460410	19460413.264312	1.72412209	1.00114441	54.328447	129.664999	72.842650	−663.763946
		±.000368	±.00000318	±.00000801	±.000213	±.000056	±.000056	±4.644041
	19460410	19460413.262573	1.72409711	1.00106980	54.327041	129.665283	72.842371	−620.496849
		±.000674	±.00000356	±.00000939	±.000428	±.000052	±.000054	±5.444341
C/1946 P1	19461027	19461026.778759	1.13610604	1.00076873	320.412716	238.335364	56.964608	−676.638371
		±.000498	±.00000296	±.00000562	±.000277	±.000188	±.000062	±4.943135
C/1946 U1	19470224	19470207.362613	2.40766593	1.00094633	348.624706	35.558527	108.174444	−393.047880
		±.000422	±.00000218	±.00001085	±.000140	±.000049	±.000048	±4.504928
	19470224	19470207.363185	2.40764364	1.00089117	348.624923	35.558720	108.174352	−370.143668
		±.000519	±.00000786	±.00001917	±.000177	±.000068	±.000051	±7.800650
C/1947 S1	19480219	19480216.423429	0.74812370	1.00035570	350.214858	271.439960	140.568349	−475.455030
		±.000066	±.00000075	±.00000258	±.000179	±.000229	±.000078	±3.453175
	19480219	19480216.422309	0.74810617	1.00023485	350.213385	271.439361	140.568516	−313.924888
		±.000138	±.00000196	±.00001240	±.000206	±.000208	±.000062	±16.575559
C/1947 Y1	19480219	19480216.691915	1.49955491	1.00108229	61.923925	199.300972	77.533200	−721.741506
		±.000266	±.00000327	±.00001286	±.000215	±.000072	±.000061	±8.577917
C/1948 E1	19480509	19480516.612175	2.10705582	1.00077771	66.898096	247.652645	92.919469	−369.095825
		±.000281	±.00000236	±.00000570	±.000124	±.000043	±.000032	±2.703396
C/1948 T1	19470912	19470904.429515	3.26110877	1.00227683	73.464822	122.120668	155.077948	−698.175954
		±.010323	±.00011350	±.00003289	±.001866	±.000217	±.000265	±10.071964
C/1950 K1	19510203	19510115.043740	2.57232857	1.00121061	192.468633	38.890330	144.155175	−470.626833
		±.000378	±.00000139	±.00000556	±.000092	±.000047	±.000031	±2.161805

Table B.2. NG parameters derived in NG orbital solutions given in Table B.1.

Comet	NG parameters defined by Eq. (2) in units of 10^{-8} AU day^{-2}			τ
	A_1	A_2	A_3	[days]
(1)	(2)	(3)	(4)	(5)
C/1906 B1	7.323 ± 1.841	–	–	–
C/1911 S3	3.930 ± 0.798	–	–	–
C/1913 Y1	1.240 ± 0.172	–	–	–
C/1914 F1	4.834 ± 0.681	4.85 ± 1.19	2.481 ± 0.826	–
C/1916 G1	2.502 ± 0.442	0.708 ± 0.363	−0.2692 ± 0.0699	–
C/1921 E1	3.155 ± 0.629	−0.451 ± 0.861	–	–
C/1937 C1	2.146 ± 0.968	−0.002 ± 0.452	–	–
C/1937 N1	1.976 ± 0.495	2.115 ± 0.883	−0.102 ± 0.193	–
C/1940 R2	1.426 ± 0.155	−0.0392 ± 0.0598	–	–
C/1942 C1	1.150 ± 0.545	−0.322 ± 0.229	−0.739 ± 0.252	–
C/1946 C1	1.857 ± 0.540	3.434 ± 0.409	–	–
C/1946 U1	13.03 ± 4.61	–	–	–
C/1947 S1	2.055 ± 0.207	−2.3409 ± 0.0649	–	–

Appendix C: Original and future barycentric inverse semi-major axes and orbit-quality assessment

Table C.1. Values of original and future barycentric, reciprocal semi-major axes in comparison to values published in MW08, and comparison of data used (Col. (3)) and orbit-quality assessment (Cols. (2) and (11)–(12)).

Comet	Marsden & Williams Catalogue (MW08)					Present Catalogue – the new results					
	MSE class	Per cent of residuals used	$1/a_{ori}$ in units of 10^{-6} AU^{-1}	$1/a_{osc}$	$1/a_{fut}$	$1/a_{ori}$ in units of 10^{-6}AU^{-1}	$1/a_{fut}$	rms [″]	No. of res.	MSE class	New class
(1)	(2)	(3)	(4)	(5)	(6)	(7)	(8)	(9)	(10)	(11)	(12)
C/1902 R1	1B	80	27	79	865	31.04 ± 1.71	870.94 ± 1.71	2.28	2501	1A	1b
C/1902 X1	1B	29	26	−218	−488	74.03 ± 7.25	−439.81 ± 7.24	1.66	1307	1B	1b
C/1903 M1	1B	45	33	−1230	−1000	24.12 ± 9.55	−1010.00 ± 9.55	2.03	1021	1B	2a
C/1904 Y1	2A	32	−75	−360	170	101. ± 117.	348. ± 117.	2.87	302	2A	2b
C/1906 B1	1B	83	−75	−857	−343	−135.59 ± 22.96	−402.66 ± 22.97	3.07	450	1B	2a
						117.32 : 73.86	−149.58 : 73.87	3.05	449	1B	2a
C/1906 E1*	1B	123	28	−452	−519	17.35 ± 5.55	−529.52 ± 5.54	1.96	812	1A	1a
C/1907 E1	1B	45	25	−489	−290	33.76 ± 21.56	−281.04 ± 21.55	2.56	296	1B	2a
C/1911 S3	2A	54	−74	−483	+175	−163.8 ± 36.8	80.7 ± 36.8	2.35	246	2A	2a
						796. : 205.	1041. : 205	2.10	244	2B	2b
C/1912 R1	1B	20	45	−630	−363	36.77 ± 5.27	−370.81 ± 5.27	2.48	1670	1B	1b
C/1913 Y1	1A	36	29	−140	063	22.14 ± 1.30	56.41 ± 1.30	2.06	1874	1A	1a
						52.57 : 4.23	86.84 : 4.23	2.00	1860	1A	1a
C/1914 F1	2A	24	126	−88	1561	57.45 ± 28.41	1492.0 ± 28.4	3.33	517	2A	2a
						600. : 152.	1475.8 : 37.7	3.12	519	2A	2b
C/1914 M1*	1A	64	27	−878	−1	36.6 ± 25.9	8.5 ± 25.0	2.21	122	1B	1b
C/1916 G1	1A	45	17	353	763	35.33 ± 3.20	781.41 ± 3.20	1.97	823	1A	1a
						69.59 : 9.48	783.75 : 8.79	1.84	817	1A	1b
C/1919 Q2	2A	35	20	−199	−42	34.7 ± 67.3	−26.9 ± 67.3	2.58	498	2A	2a
C/1921 E1	1B	32	18	−354	−351	−120.1 ± 37.6	−488.8 ± 37.4	3.27	914	1B	2a
						85.9 : 80.8	−210.9 : 96.6	3.25	914	1B	2a
C/1922 U1	1A	45	21	−334	−523	2.35 ± 8.52	−542.13 ± 8.51	1.82	826	1A	1b
C/1925 F1*	1A	25	35	−582	128	34.83 ± 8.45	127.96 ± 8.45	2.75	463	1A	1b
C/1925 G1	1A	42	40	−545	−533	40.03 ± 5.74	−532.49 ± 5.74	2.79	964	1A	1b
C/1925 W1	1B	44	24	−244	−322	28.59 ± 9.62	−317.76 ± 9.61	1.94	593	1B	1b
C/1932 M1	1B	30	−56	−365	−327	24.21 ± 19.40	−245.8 ± 19.4	2.60	325	1B	1b
C/1932 M2	1A	59	45	−619	−240	56.58 ± 3.07	−229.01 ± 3.07	1.77	546	1A	1a
C/1935 Q1*	1A	86	19	−506	−281	13.16 ± 5.19	−285.68 ± 5.19	1.49	250	1A	1a
C/1937 C1	1B	35	62	−79	1400	58.40 ± 7.16	1396.88 ± 7.17	2.53	767	1B	1b
						44.8 : 14.4	1383.3 : 11.7	2.48	766	1B	1b
C/1937 N1	2A	55	124	17	281	37.3 ± 40.5	194.2 ± 40.5	2.05	765	2A	2a
						507. : 101.	231. : 172.	1.92	766	2A	2a
C/1940 R2	1B	56	1	−1319	−1570	−60.0 ± 17.7	−1630.6 ± 17.7	1.77	678	1B	1b
						51.6 : 17.1	−1494.0 : 35.7	1.49	670	1B	1b
C/1940 S1	2B	62	−124	−1374	−1123	297. ± 427.	−703. ± 427.	3.67	61	2A	2b
C/1941 K1	1B	79	78	−278	190	53.89 ± 2.47	166.22 ± 2.47	2.22	801	1A	1b
C/1942 C1	1B	111	16	−618	−821	22.60 ± 3.33	−813.98 ± 3.33	1.46	412	1A	1a
						37.0 : 15.6	−775.68 : 8.58	1.23	411	1A	1b
C/1942 C2*	1A	80	−34	−774	−282	−29.1 ± 13.5	−278.3 ± 13.5	1.57	88	1A	1b
C/1944 K2	1A	89	18	−937	−522	20.8 ± 12.8	−518.7 ± 12.8	1.58	56	1A	1b
C/1946 C1	1A	43	−13	−678	373	0.80 ± 4.60	386.97 ± 4.60	2.54	857	1A	1a
						102.4 : 12.7	346.80 : 5.61	2.17	848	1A	1b
C/1946 P1	1A	79	44	−683	16	50.86 ± 5.08	22.55 ± 5.08	0.99	257	1A	1a
C/1946 U1	1A	75	−1	−393	26	−0.59 ± 4.54	26.22 ± 4.54	1.25	259	1A	1a
						17.08 : 6.52	43.88 : 6.52	1.19	259	1B	1b
C/1947 S1	1A	45	24	−485	−366	33.34 ± 3.46	−356.31 ± 3.46	2.59	546	1A	1a
						53.02 : 8.19	−277.6 : 11.7	2.42	543	1A	1b
C/1947 Y1	1B	76	28	−724	53	28.89 ± 8.49	54.31 ± 8.50	1.22	204	1B	1b
C/1948 E1	1A	44	34	−373	31	37.25 ± 2.74	35.21 ± 2.74	1.48	431	1A	1a
C/1948 T1*	1A	100	34	−699	225	34.2 ± 10.0	225.0 ± 10.0	0.94	52	1A	1b
C/1950 K1	1A	16	37	−479	270	45.1 ± 2.2	278.4 ± 2.2	1.28	466	1A	1a

Notes. Columns (4)–(6) show values of $1/a_{ori}$, $1/a_{osc}$ and $1/a_{fut}$ taken from MW08, Cols. (7)–(8) give values of $1/a_{ori}$ and $1/a_{fut}$ and their uncertainties derived in the present investigation. NG solutions are given in the second row of these comets when these solutions were possible to determine. The rms and the number of residuals are additionally given in Cols. (9)–(10). In the last two columns the quality class assessments are presented using the standard MSE method (Col. (12)), and the new revised method proposed by Królikowska & Dybczyński (Col. (13)). Column (3) shows the per cent of residuals used in MW08 in comparison to residuals used here for each comet (compare Col. (10) with twice as many as given in Col. (9) of Table A.1). NG models are indicated by light grey shading, an asterisk in Col. (1) indicates comets with large perihelion distances. For more details see the text.

Appendix D: Original barycentric orbital elements

Table D.1. Orbital elements of original barycentric orbits, that is, before entering the planetary zone for all models described in Table C.1.

Comet	Epoch	T	q	e	ω	Ω	i	$1/a_{\rm ori}$
	[yyyymmdd]	[yyyymmdd.dddddd]	[AU]		[°]	[°]	[°]	[10^{-6} AU^{-1}]
(1)	(2)	(3)	(4)	(5)	(6)	(7)	(8)	(9)
C/1902 R1	16050616	19021124.748046	0.39752997	0.99998766	152.968369	50.636389	156.486711	31.04
		±0.000042	±0.00000028	±0.00000067	±0.000084	±0.000087	±0.000040	±1.71
C/1902 X1	16010128	19030324.059433	2.77648897	0.99979445	5.819304	118.884571	43.892926	74.03
		±0.002493	±0.00001348	±0.00002012	±0.000769	±0.000087	±0.000261	±7.25
C/1903 M1	16060611	19030826.871477	0.32438523	0.99999218	127.495100	294.778173	85.303818	24.12
		±0.000043	±0.00000159	±0.00000310	±0.000266	±0.000054	±0.000202	±9.55
C/1904 Y1	16031204	19041103.420926	1.88656503	0.99980792	40.672000	219.740942	99.546209	101.81
		±0.013759	±0.00009818	±0.00022132	±0.006737	±0.000570	±0.000554	±117.32
C/1906 B1	16081107	19051222.176515	1.29645026	1.00017579	89.834094	287.548057	126.511964	−135.59
		±0.000916	±0.00000337	±0.00002976	±0.000348	±0.000302	±0.000197	±22.96
	16060102	19051222.173035	1.29627992	0.99984792	89.843280	287.549903	126.512022	117.32
		±0.001408	±0.00004429	±0.00009573	±0.002419	±0.000595	±0.000192	±73.86
C/1906 E1	16030518	19051017.833416	3.33691190	0.99994209	158.570127	343.735716	4.287970	17.35
		±0.001867	±0.00001423	±0.00001852	±0.000818	±0.000732	±0.000190	±5.55
C/1907 E1	16061012	19070320.532327	2.05146625	0.99993073	317.181114	98.439032	141.685157	33.76
		±0.001520	±0.00001619	±0.00004422	±0.000820	±0.000215	±0.000201	±21.55
C/1911 S3	16160817	19111010.212422	0.30444763	1.00004987	71.678698	89.139025	96.440241	−163.80
		±0.000557	±0.00000077	±0.00001120	±0.000389	±0.000420	±0.000553	±36.80
	16050616	19111010.198180	0.30444215	0.99975759	71.680473	89.140777	96.445791	796.26
		±0.003218	±0.00000134	±0.00006235	±0.000499	±0.000521	±0.001329	±204.81
C/1912 R1	16140828	19121004.999276	0.71382525	0.99997375	25.719944	298.264840	79.846805	36.77
		±0.000056	±0.00000082	±0.00000376	±0.000110	±0.000112	±0.000085	±5.27
C/1913 Y1	16160310	19141025.816829	1.10070306	0.99997563	97.539554	60.475762	67.986327	22.14
		±0.000055	±0.00000079	±0.00000143	±0.000028	±0.000024	±0.000043	±1.30
	16151111	19141025.817363	1.10067114	0.99994214	97.541763	60.475772	67.986634	52.57
		±0.000089	±0.00000460	±0.00000465	±0.000303	±0.000024	±0.000059	±4.23
C/1914 F1	16150425	19140604.671419	1.20014864	0.99993105	72.188980	200.123181	23.910787	57.45
		±0.000268	±0.00000515	±0.00003410	±0.000265	±0.000308	±0.000343	±28.41
	16081107	19140604.688500	1.19991017	0.99928025	72.209576	200.117596	23.903136	599.84
		±0.003739	±0.00005139	±0.00018235	±0.004142	±0.001699	±0.002255	±151.99
C/1914 M1	16110225	19140730.529118	3.74227102	0.99986307	14.115408	271.473680	71.078722	36.59
		±0.010705	±0.00006815	±0.00009344	±0.002097	±0.000169	±0.000424	±24.97
C/1916 G1	16170921	19170617.357661	1.69219889	0.99994022	120.502725	184.485105	25.605811	35.33
		±0.000249	±0.00000105	±0.00000541	±0.000140	±0.000054	±0.000045	±3.20
	16170414	19170617.362353	1.69214922	0.99988224	120.505372	184.485407	25.605536	69.59
		±0.001103	±0.00000924	±0.00001603	±0.000640	±0.000122	±0.000064	±9.48
C/1919 Q2	16210324	19191207.325501	1.11815172	0.99996124	185.698259	122.175370	46.404177	34.67
		±0.002308	±0.00002761	±0.00007521	±0.002474	±0.000564	±0.000178	±67.26
C/1921 E1	16240706	19210510.690297	1.00693074	1.00012096	64.705467	269.587562	132.180302	−120.12
		±0.000189	±0.00000143	±0.00003788	±0.000237	±0.000307	±0.000115	±37.62
	16220319	19210510.691603	1.00687747	0.99991349	64.710041	269.585493	132.181074	85.92
		±0.001631	±0.00002269	±0.00008135	±0.002464	±0.000538	±0.000188	±80.79
C/1922 U1	16220607	19221025.586946	2.25655127	0.99999470	118.331242	221.632968	51.422827	2.35
		±0.001413	±0.00000784	±0.00001923	±0.000480	±0.000056	±0.000036	±8.52
C/1925 F1	16210722	19250906.261864	4.17819249	0.99985439	205.622401	358.368841	146.741752	34.85
		±0.003957	±0.00002339	±0.00003480	±0.000574	±0.000093	±0.000145	±8.33
C/1925 G1	16260626	19250331.956264	1.10542489	0.99995575	36.344786	319.188844	100.089542	40.03
		±0.000268	±0.00000304	±0.00000635	±0.000283	±0.000060	±0.000081	±5.75
C/1925 W1	16260407	19251002.714744	1.56532856	0.99995524	106.401280	335.706396	49.270625	28.59
		±0.000382	±0.00001534	±0.00001506	±0.000599	±0.000041	±0.000414	±9.62
C/1932 M1	16330301	19320923.758305	1.64447847	0.99996018	69.867810	246.157067	78.369050	24.21
		±0.001011	±0.00001183	±0.00003190	±0.000641	±0.000228	±0.000199	±19.40
C/1932 M2	16310819	19320921.542393	2.31250621	0.99986916	329.793942	216.089015	125.023427	56.58
		±0.000469	±0.00000275	±0.00000711	±0.000144	±0.000057	±0.000050	±3.07
C/1935 Q1	16320922	19360511.115435	4.03419814	0.99994692	45.035086	300.599583	66.129296	13.16
		±0.001724	±0.00000987	±0.00002094	±0.000250	±0.000060	±0.000051	±5.19
C/1937 C1	16370429	19370620.221049	1.73545046	0.99989864	107.714649	128.591694	41.523168	58.40

Notes. The successive columns signify (1) – comet designation; (2) – epoch, that is, osculation date; (3) – perihelion time [TT]; (4) – perihelion distance; (5) – eccentricity; (6) – argument of perihelion (in degrees), equinox 2000.0; (7) – longitude of the ascending node (in degrees), equinox 2000.0; (8) – inclination (in degrees), equinox 2000.0; (9) – reciprocal original semi-major axis in units of 10^{-6} AU^{-1}. Original orbits determined using the NG model of motion are indicated by light grey shading.

Table D.1. continued.

Comet	Epoch	T	q	e	ω	Ω	i	$1/a_{\rm ori}$
	[yyyymmdd]	[yyyymmdd.dddddd]	[AU]		[°]	[°]	[°]	[10^{-6} AU^{-1}]
(1)	(2)	(3)	(4)	(5)	(6)	(7)	(8)	(9)
		±0.000506	±0.00000397	±0.00001243	±0.000300	±0.000109	±0.000084	±7.16
	16370718	19370620.222929	1.73543405	0.99992220	107.716372	128.591468	41.523205	44.83
		±0.000968	±0.00000793	±0.00002491	±0.000841	±0.000156	±0.000090	±14.36
C/1937 N1	16390419	19370815.655572	0.85943419	0.99996793	114.977962	59.471335	146.361452	37.31
		±0.001324	±0.00000041	±0.00003482	±0.000370	±0.000201	±0.000205	±40.51
	16331027	19370815.661527	0.85934606	0.99956398	114.991035	59.472210	146.363379	507.39
		±0.001656	±0.00002184	±0.00008654	±0.002703	±0.000809	±0.000573	±100.71
C/1940 R2	16440830	19410115.973517	0.36427644	1.00002186	199.546182	296.892318	50.185071	−60.01
		±0.000159	±0.00000282	±0.00000646	±0.000115	±0.000141	±0.000168	±17.74
	16430617	19410115.973647	0.36427385	0.99998121	199.547949	296.892704	50.184132	51.59
		±0.000186	±0.00000275	±0.00000624	±0.000223	±0.000181	±0.000151	±17.12
C/1940 S1	16381220	19400816.604848	1.06507308	0.99968363	329.678357	128.069124	133.275676	297.04
		±0.016026	±0.00043374	±0.00045458	±0.037243	±0.006470	±0.000940	±426.92
C/1941 K1	16430217	19410903.211543	0.87864337	0.99995265	85.289643	257.546307	94.468456	53.89
		±0.000061	±0.00000031	±0.00000217	±0.000038	±0.000024	±0.000108	±2.47
C/1942 C1	16430217	19420430.110680	1.44096429	0.99996744	223.544907	341.080318	79.489648	22.60
		±0.000112	±0.00000076	±0.00000481	±0.000077	±0.000017	±0.000063	±3.33
	16430108	19420430.111719	1.44094260	0.99994665	223.546319	341.080424	79.488513	37.02
		±0.000984	±0.00001325	±0.00002241	±0.001010	±0.000038	±0.000463	±15.55
C/1942 C2	16390708	19420928.842884	4.10696133	1.00011952	163.752994	281.002773	172.517772	−29.10
		±0.007726	±0.00003147	±0.00005531	±0.001446	±0.000850	±0.000123	±13.47
C/1944 K2	16440105	19440718.501473	2.22564815	0.99995373	337.096904	203.525912	95.124917	20.79
		±0.001683	±0.00001298	±0.00002854	±0.000687	±0.000191	±0.000157	±12.82
C/1946 C1	16461108	19460412.084826	1.71681103	0.99999862	54.466561	129.577886	72.875740	0.80
		±0.000713	±0.00000306	±0.00000789	±0.000212	±0.000055	±0.000056	±4.60
	16450825	19460412.089411	1.71675231	0.99982419	54.469479	129.578179	72.875457	102.41
		±0.000901	±0.00000645	±0.00002185	±0.000666	±0.000053	±0.000055	±12.73
C/1946 P1	16471103	19461026.493829	1.12948754	0.99994255	320.574302	238.295327	57.042068	50.86
		±0.000520	±0.00000300	±0.00000573	±0.000286	±0.000193	±0.000064	±5.07
C/1946 U1	16460601	19470206.851120	2.41089055	1.00000141	348.604392	35.566639	108.115380	−0.59
		±0.000555	±0.00000216	±0.00001094	±0.000140	±0.000048	±0.000048	±4.54
	16460422	19470206.857997	2.41085327	0.99995883	348.607122	35.566834	108.115289	17.08
		±0.002586	±0.00001313	±0.00001572	±0.001023	±0.000069	±0.000051	±6.52
C/1947 S1	16500111	19480217.010780	0.74919707	0.99997502	350.249194	271.413569	140.601343	33.34
		±0.000061	±0.00000076	±0.00000259	±0.000181	±0.000231	±0.000079	±3.46
	16491023	19480217.009294	0.74915527	0.99996030	350.251157	271.412966	140.601506	52.99
		±0.000304	±0.00000502	±0.00000614	±0.000340	±0.000207	±0.000062	±8.20
C/1947 Y1	16481028	19480215.276061	1.49138818	0.99995691	62.089047	199.256479	77.586851	28.89
		±0.000370	±0.00000319	±0.00001267	±0.000218	±0.000073	±0.000061	±8.49
C/1948 E1	16471103	19480515.582710	2.09496271	0.99992197	67.168988	247.706993	92.925547	37.25
		±0.000303	±0.00000240	±0.00000575	±0.000127	±0.000044	±0.000034	±2.74
C/1948 T1	16450206	19470903.743055	3.26052435	0.99988853	73.395315	121.990438	155.123775	34.19
		±0.010324	±0.00011080	±0.00003277	±0.001840	±0.000217	±0.000260	±10.05
C/1950 K1	16490804	19510115.032274	2.57130432	0.99988404	192.367874	38.749976	144.145001	45.10
		±0.000373	±0.00000141	±0.00000560	±0.000093	±0.000047	±0.000031	±2.18

Appendix E: Future barycentric orbital elements

Table E.1. Orbital elements of future barycentric orbits, that is, after suffering the planetary perturbations for all models described in Table C.1.

Comet	Epoch	T	q	e	ω	Ω	i	$1/a_{\rm fut}$
	[yyyymmdd]	[yyyymmdd.dddddd]	[AU]		[°]	[°]	[°]	[10^{-6} AU^{-1}]
(1)	(2)	(3)	(4)	(5)	(6)	(7)	(8)	(9)
C/1902 R1	22100426	19021124.008464	0.40184116	0.99965002	152.815403	50.627736	156.403506	870.94
		±0.000019	±0.00000033	±0.00000069	±0.000086	±0.000088	±0.000037	±1.71
C/1902 X1	21990801	19030323.651406	2.78159684	1.00122340	5.932702	118.796694	43.858159	−439.82
		±0.002538	±0.00001339	±0.00002014	±0.000770	±0.000085	±0.000262	±7.24
C/1903 M1	21900120	19030828.359623	0.33314041	1.00033647	127.333709	295.030879	84.934214	−1010.01
		±0.000136	±0.00000153	±0.00000318	±0.000266	±0.000058	±0.000200	±9.55
C/1904 Y1	22080725	19041104.322846	1.88304686	0.99934541	40.729565	219.768501	99.640020	347.62
		±0.013289	±0.00010131	±0.00022098	±0.006727	±0.000580	±0.000593	±117.37
C/1906 B1	22000329	19051224.093101	1.28893207	1.00051887	89.763925	287.836952	126.593908	−402.56
		±0.000459	±0.00000338	±0.00002960	±0.000344	±0.000313	±0.000199	±22.96
	22021224	19051224.081525	1.28876275	1.00019277	89.750691	287.838945	126.593965	−149.58
		±0.003074	±0.00004399	±0.00009521	±0.003441	±0.000635	±0.000194	±73.87
C/1906 E1	22020319	19051017.757182	3.34445809	1.00177097	158.629204	343.663142	4.280140	−529.52
		±0.001897	±0.00001428	±0.00001853	±0.000819	±0.000733	±0.000190	±5.54
C/1907 E1	22040131	19070320.176742	2.04521487	1.00057480	317.069049	98.573559	141.673192	−281.04
		±0.001723	±0.00001627	±0.00004407	±0.000814	±0.000221	±0.000193	±21.54
C/1911 S3	22090720	19111011.596948	0.30043610	0.99997575	71.589527	89.279608	96.563646	80.70
		±0.000548	±0.00000079	±0.00001106	±0.000386	±0.000422	±0.000553	±36.80
	22210227	19111011.613216	0.30042613	0.99968737	71.591551	89.281396	96.569195	1040.62
		±0.003643	±0.00000226	±0.00006152	±0.000534	±0.000529	±0.001329	±204.78
C/1912 R1	22060517	19121005.284559	0.71584674	1.00026544	25.598506	298.263151	79.808281	−370.81
		±0.000055	±0.00000088	±0.00000377	±0.000110	±0.000111	±0.000084	±5.27
C/1913 Y1	22131027	19141026.924754	1.10518625	0.99993766	97.460986	60.292940	67.982189	56.41
		±0.000074	±0.00000079	±0.00000143	±0.000028	±0.000024	±0.000043	±1.30
	22140224	19141026.924707	1.10515434	0.99990403	97.458874	60.292937	67.982497	86.84
		±0.000072	±0.00000460	±0.00000467	±0.000300	±0.000023	±0.000059	±4.23
C/1914 F1	22310903	19140605.374133	1.18818561	0.99822733	71.900648	200.113641	23.956594	1491.91
		±0.000210	±0.00000581	±0.00003377	±0.000279	±0.000334	±0.000349	±28.43
	22310506	19140605.383588	1.18811153	0.99824831	71.895811	200.118493	23.950336	1474.34
		±0.002600	±0.00001532	±0.00004474	±0.001262	±0.001861	±0.001799	±37.67
C/1914 M1	22170827	19140730.313104	3.74262397	0.99996809	13.874513	271.460496	71.079539	8.53
		±0.010833	±0.00006880	±0.00009356	±0.002108	±0.000169	±0.000423	±25.00
C/1916 G1	22260313	19170618.004132	1.68486080	0.99868344	120.734220	184.255647	25.636610	781.41
		±0.000249	±0.00000104	±0.00000539	±0.000142	±0.000054	±0.000045	±3.20
	22260313	19170618.002781	1.68482103	0.99867953	120.732445	184.255375	25.636480	783.75
		±0.000285	±0.00000571	±0.00001481	±0.000275	±0.000066	±0.000079	±8.79
C/1919 Q2	22171225	19191208.123284	1.11801549	1.00003007	185.783020	122.055357	46.365671	−26.89
		±0.002011	±0.00002841	±0.00007526	±0.002443	±0.000557	±0.000179	±67.31
C/1921 E1	22140224	19210510.725714	1.00362490	1.00049067	64.338847	269.351069	132.108442	−488.90
		±0.000333	±0.00000145	±0.00003778	±0.000239	±0.000282	±0.000123	±37.64
	22170320	19210510.725850	1.00355226	1.00021161	64.332073	269.349172	132.109300	−210.87
		±0.001774	±0.00002192	±0.00009696	±0.002369	±0.000497	±0.000210	±96.61
C/1922 U1	22170320	19221026.356621	2.26579397	1.00122836	118.400924	221.526423	51.410666	−542.13
		±0.001274	±0.00000754	±0.00001929	±0.000480	±0.000054	±0.000035	±8.51
C/1925 F1	22301127	19250905.761751	4.18479767	0.99946443	205.679732	358.527886	146.715638	127.98
		±0.004022	±0.00002335	±0.00003486	±0.000573	±0.000097	±0.000144	±8.33
C/1925 G1	22171006	19250401.599089	1.10790258	1.00058995	36.149443	319.121445	99.886189	−532.49
		±0.000224	±0.00000311	±0.00000637	±0.000282	±0.000059	±0.000081	±5.74
C/1925 W1	22210518	19251003.313123	1.56877876	1.00049850	106.484194	335.500024	49.276562	−317.76
		±0.000286	±0.00001517	±0.00001508	±0.000597	±0.000042	±0.000414	±9.61
C/1932 M1	22290406	19320924.831765	1.64649976	1.00040467	69.763011	246.059025	78.330249	−245.77
		±0.001018	±0.00001203	±0.00003194	±0.000641	±0.000225	±0.000200	±19.40
C/1932 M2	22300730	19320921.652251	2.30775841	1.00052850	329.645277	216.182491	125.017993	−229.01
		±0.000480	±0.00000273	±0.00000709	±0.000144	±0.000058	±0.000050	±3.07
C/1935 Q1	22360807	19360511.495408	4.03970045	1.00115405	44.839534	300.607693	66.119413	−285.68
		±0.001671	±0.00000994	±0.00002096	±0.000252	±0.000060	±0.000051	±5.19
C/1937 C1	22540505	19370620.739997	1.71646743	0.99760231	107.371079	128.427941	41.478490	1396.88

Notes. The successive columns signify (1) – comet designation; (2) – epoch, that is, osculation date; (3) – perihelion time [TT]; (4) – perihelion distance; (5) – eccentricity; (6) – argument of perihelion (in degrees), equinox 2000.0; (7) – longitude of the ascending node (in degrees), equinox 2000.0; (8) – inclination (in degrees), equinox 2000.0; (9) – reciprocal future semi-major axis in units of 10^{-6} AU^{-1}. Future orbits determined using the NG model of motion are indicated by light grey shading.

Table E.1. continued.

Comet	Epoch	T	q	e	ω	Ω	i	$1/a_{\rm fut}$
	[yyyymmdd]	[yyyymmdd.dddddd]	[AU]		[°]	[°]	[°]	[10^{-6} AU^{-1}]
(1)	(2)	(3)	(4)	(5)	(6)	(7)	(8)	(9)
		±0.000458	±0.00000408	±0.00001230	±0.000299	±0.000104	±0.000083	±7.17
	22540326	19370620.736751	1.71645095	0.99762556	107.368860	128.427721	41.478508	1383.34
		±0.001577	±0.00001050	±0.00002006	±0.001035	±0.000152	±0.000087	±11.69
C/1937 N1	22370911	19370815.710412	0.85988734	0.99983290	114.636164	59.325102	146.421365	194.32
		±0.000147	±0.00000043	±0.00003483	±0.000405	±0.000235	±0.000195	±40.51
	22380218	19370815.715783	0.85990802	0.99980114	114.641669	59.325890	146.423252	231.25
		±0.001815	±0.00002536	±0.00014765	±0.002542	±0.000772	±0.000625	±171.71
C/1940 R2	22210806	19410115.372565	0.37020628	1.00060367	199.642916	296.590685	49.670477	−1630.62
		±0.000073	±0.00000271	±0.00000657	±0.000117	±0.000141	±0.000171	±17.75
	22221129	19410115.373155	0.37020004	1.00055310	199.639408	296.591043	49.669507	−1494.06
		±0.000183	±0.00000311	±0.00001323	±0.000646	±0.000184	±0.000154	±35.72
C/1940 S1	22310506	19400816.426110	1.05927916	1.00074474	329.790299	128.282572	133.042273	−703.06
		±0.020134	±0.00042718	±0.00045228	±0.036971	±0.006163	±0.001158	±426.69
C/1941 K1	22410712	19410904.986298	0.86551738	0.99985613	85.103947	257.564985	94.558245	166.22
		±0.000077	±0.00000031	±0.00000213	±0.000038	±0.000024	±0.000108	±2.47
C/1942 C1	22320719	19420430.287518	1.44687232	1.00117778	223.445496	340.917068	79.307804	−814.02
		±0.000120	±0.00000079	±0.00000482	±0.000077	±0.000017	±0.000063	±3.33
	22321226	19420430.286227	1.44684302	1.00112229	223.443680	340.917930	79.307463	−775.68
		±0.000390	±0.00001091	±0.00001243	±0.000555	±0.000293	±0.000203	±8.59
C/1942 C2	22430304	19420925.248677	4.10166979	1.00114131	163.296372	281.066902	172.512207	−278.26
		±0.007699	±0.00003144	±0.00005528	±0.001447	±0.000849	±0.000123	±13.47
C/1944 K2	22390215	19440718.115518	2.22184587	1.00115253	336.928234	203.612746	94.989126	−518.73
		±0.001858	±0.00001318	±0.00002848	±0.000683	±0.000193	±0.000156	±12.82
C/1946 C1	22500307	19460412.859596	1.72038322	0.99933427	54.182409	129.696232	72.941443	386.97
		±0.000352	±0.00000321	±0.00000791	±0.000211	±0.000055	±0.000056	±4.60
	22490928	19460412.860782	1.72036623	0.99940339	54.181924	129.696514	72.941172	346.80
		±0.000603	±0.00000764	±0.00000964	±0.000402	±0.000053	±0.000055	±5.61
C/1946 P1	22450621	19461026.922779	1.13244087	0.99997447	320.262683	238.420478	56.958209	22.55
		±0.000509	±0.00000300	±0.00000575	±0.000284	±0.000193	±0.000063	±5.08
C/1946 U1	22471228	19470207.503759	2.41255932	0.99993675	348.625816	35.533705	108.158906	26.22
		±0.000434	±0.00000210	±0.00001094	±0.000140	±0.000048	±0.000048	±4.54
	22480317	19470207.500365	2.41252207	0.99989415	348.624376	35.533900	108.158812	43.88
		±0.001228	±0.00001314	±0.00001573	±0.000512	±0.000069	±0.000051	±6.52
C/1947 S1	22411219	19480216.805182	0.74487969	1.00026541	350.247822	271.579999	140.472078	−356.31
		±0.000086	±0.00000076	±0.00000258	±0.000181	±0.000231	±0.000079	±3.46
	22420925	19480216.803521	0.74482539	1.00020675	350.241846	271.579407	140.472235	−277.59
		±0.000310	±0.00000550	±0.00000870	±0.000620	±0.000206	±0.000061	±11.68
C/1947 Y1	22471009	19480216.304140	1.49784258	0.99991866	61.829573	199.327504	77.567907	54.31
		±0.000211	±0.00000338	±0.00001273	±0.000217	±0.000072	±0.000061	±8.50
C/1948 E1	22481112	19480516.423445	2.10546507	0.99992587	66.831432	247.667975	92.893283	35.21
		±0.000277	±0.00000244	±0.00000577	±0.000127	±0.000044	±0.000033	±2.74
C/1948 T1	22520624	19470903.674841	3.27021985	0.99926416	73.548717	122.147554	155.105084	225.01
		±0.010358	±0.00011088	±0.00003285	±0.001821	±0.000214	±0.000259	±10.05
C/1950 K1	22550321	19510114.572471	2.57371784	0.99928354	192.416020	38.885979	144.138428	278.37
		±0.000396	±0.00000139	±0.00000561	±0.000093	±0.000048	±0.000031	±2.18